8.1.2.8 Zunyite, davreuxite, keldyshite, gageite, pumpellyite, jennite and related silicates

The above sorosilicates classified in groups VIIIB20-VIIIB28, according to the Mineral Reference Manual [91N1] are listed in Table 1.

8.1.2.8.1 Crystal structures. Lattice parameters

Zunyite

The crystal structure of zunyite, $Al_{13}Si_5O_{20}(OH,F)_{18}Cl$ was described by [33P1] and refined later by [60K1, 62T1, 73L1, 82B1]. The last report gives a systematic description of this complicated structure. The silicate crystallizes in space group $F\bar{4}3m$. The structure consists of two crystallographic units, a Si_5O_{16} pentamer and a group of the Keggin molecule type [92F1] with $^{[4]}Al^{[6]}Al_{12}O_{16}(OH)_{24}$ stoichiometry. The Keggin molecule-type group is a dimensionally constant unit of the $Al_{13}O_{16}(OH)_{18}$ framework. The structure can be described following the Chieh approach [80C1]. While [80C1] prefers to use polyhedra outlined by the atoms closest to the fourfold sets of equivalent sites of symmetry $\bar{4}3m$, in [82B1] the chemically relevant geometric units were emphasized. In space group $F\bar{4}3m$ there are four such sets, A, C, B, D, named after Wyckoff notation, and listed in ascending order along the body diagonal of the cube: A in 000; C in 1/4, 1/4, 1/4; B in 1/2, 1/2, 1/2 and D in 3/4, 3/4, 3/4 [82B1]. Set A itself is not occupied in zunyite. It is surrounded in tetrahedral fashion by four $Al_3O_4(OH)_9$ groups which all share two of their OH corners with each of the neighboring trimers to form the $Al_{12}O_{16}(OH)_{30}$ clusters centered on A. These clusters in turn share OH vertices to form an octahedral framework of composition $Al_{12}O_{16}(OH)_{18}$. Since set A by itself is arranged in the face-centered cubic pattern, each $Al_{12}O_{16}(OH)_{18}$ cluster is connected to twelve such neighboring clusters and it shares two corners with each of them. The pentameric Si_5O_{16} unit is centered on set C. It shares O atoms with the octahedral framework. The relative arrangement of A and C clusters is identical to the array of Zn and S in the zincblende type. The zincblende-type framework has the composition $Si_5Al_{12}O_{20}(OH)_{18}$ and is further interconnected by tetrahedral AlO_4 units in set D which likewise share O atoms with the octahedral framework. The resulting octahedral-tetrahedral framework $^{[4]}Si_5{}^{[4]}Al^{[6]}Al_{12}O_{20}(OH)_{18}$ is charge balanced by Cl^- ions located in set B, each of which receives six hydrogen bonds to form hydroxyl groups $Oh3H_2$ belonging to the octahedral framework. The overall chemical formula is therefore $Si_5Al_{13}O_{20}(OH)_{18}Cl$ [33P1]. The atomic sites and isotropic thermal parameters are listed in Table 2. In Table 3 the geometric units are given, while in Table 4 the lattice parameters are presented. The Si_5O_{16} pentamer is plotted in Fig. 1.

Davreuxite

The crystal structure of *davreuxite* $MnAl_6Si_4O_{17}(OH)_2$, was analysed by [76F1, 84F1, 84S1]. The silicate crystallizes in a monoclinic-type structure having space group $P2_1/m$. Fig. 2 shows a projection of the structure down [010]. Si4 and Al2 - Table 2 - alternate in double chains of tetrahedra parallel to, and near to [010]. Si3 and Al1 alternate in single chains of tetrahedra also parallel to [010]. Si1 and Si2 form $Si_2O_6(OH)$ groups near the center of the cell. These structural elements are connected by Mn (which shows distorted 6-fold coordination) and by columns of Al3 and Al4 octahedra parallel to [010] [84S1].

Keldyshite, parakeldyshite, khibinskite

Keldyshite has the composition $NaZrSi_2O_6(OH)$ [62G1, 91N1]. The silicate crystallizes in a triclinic lattice having (probably) space group $P\bar{1}$ [69K1]. *Parakeldyshite*, $Na_2ZrSi_2O_7$, crystallizes in a triclinic lattice having space group P1 [73K1] or $P\bar{1}$ [77R1]. *Khibinskite*, $K_2ZrSi_2O_7$, is monoclinic or triclinic [73K1]. There are pronounced pseudoperiods $a' = a/2$, $b' = b/2$ and $c' = c/2$. The mineral is nearly trigonal, $\bar{3}m$ [73K1].

Tiragalloite, medaite

Tiragalloite, $Mn_4[AsSi_3O_{12}(OH)]$ crystallizes in a monoclinic-type structure having space group $P2_1/n$ [79G1, 80G1]. The characteristic feature of the crystal structure is the presence of an arsenatotrisilicate ion $(AsSi_3O_{12}OH)^{8-}$, comprising four tetrahedra linked together to form a chain fragment. This ion is an extension of the trisilicate $(Si_3O_{10})^{8-}$ ion with an additional As-centered tetrahedron linked to it.

Medaite, $Mn_6[VSi_5O_{18}(OH)]$ crystallizes also in a monoclinic-type lattice having space group $P2_1/n$ [81G1, 82G1]. Similar with tiragalloite the characteristic feature is the presence of the vanadatopentasilicate anion $[VSi_5O_{18}(OH)]^{12-}$ with some substitution of As for V. This comprises six tetrahedra linked together to form a chain fragment - Fig. 3. The conformation of the vanadatopentasilicate ion can be almost exactly derived from the corresponding arsenatotrisilicate by repeating twice the last two tetrahedra centered on Si atoms (opposite to the As ion). In view of this analogy, and of the similarity between As–O and V–O bonds, the partial substitution of the V atom by As is not surprising. A limited substitution of the As atom by V in tiragalloite has also been detected [80G1] and the two minerals occur in close association with each other.

Gageite, balangeroite, harstigite

Gageite, $Mn_{21}O_3(Si_4O_{12})_2(OH)_{20}$, is a fibrous manganese silicate. Although the complete structure determination was hampered by the disordered nature of the material, [69M1] was able to outline a substructure with reference to an orthorhombic cell with a = 13.79 Å, b = 13.68 Å, and c' = 3.279 Å, space group Pnnm ($a \times b \times c'$), disregarding the indications for a trebled c parameter that were suggested by the occurrence of additional diffuse and weak reflections. The positional and thermal parameters for all the atoms, together with the occupancies of Mn and Mg in the M1 and M2 octahedral sites of gageite[13)], refined in space group Pnnm, are given in Table 2c [87F1]. The substructure consists of two kinds of interlinked modules, both of which are built up by chains of edge-sharing octahedra: walls three chains wide (3×1 walls) and bundles that extend two chains both in width and thickness (2×2 bundles). Each module shares its free corners with the doubly shared corners of the other module. The resulting octahedral framework contains [001] pipelike channels that according to [69M1] house disordered silicate tetrahedra. Although the topology of the octahedral framework seemed to be quite well defined, the proposed number and the disordered arrangement of the tetrahedra in the channels were probably an artifact of the assumed substructure. In [79D1] was derived, on the basis of chemical analyses, $(Mg,Mn,Zn)_{40}Si_{15}O_{50}(OH)_{40}$ as the chemical content of the cell, with trembled c parameter; this emperical formula does not agree with the crystal-chemical formula $(Mn,Mg,Zn)_{42}(Si_{12}O_{36})[O_6(OH)_{48}]$ proposed by [69M1]. In [83C1] was described the fibrous silicate, *balangeroite*, the Mg-dominant analogue of gageite. From [001] rotation photographs which indicated a trembled c parameter, a ($a \times b \times c$) basic cell was obtained with c = 9.65 Å. On the basis of chemical data for balangeroite and taking into account both the structure models [69M1] and empirical formula [79D1] for gageite, the unit cell content $(Mg,Fe,Mn,)_{42}Si_{15}(O,OH)_{90}$ was proposed. Later on [87F1], the interpretations of the crystal structures of gageite and balangeroite were refined as well as their polytypic relationship, and the order-disorder phenomena in the whole structural family were considered in more general terms. Assuming sixteen Si atoms in the $a \times b \times c$ volume the formulas obtained for gageite and belangeroite are $M_{42}O_6(OH)_{40}(T_4O_{12})_4$ [87F1]. Such formula pointed to the presence of four-repeat silicate chains (T), running in the channels of the octahedral framework described by [69M1] and placed on both sides of octahedral walls (**O**) to give rise to composite T-**O**-T modules interconnected through octahedral bundles . In the above formula M are cations in octahedral coordination, mainly Mg in balangeroite and Mn in gageite. A monoclinic unit cell was evidenced in case of balangeroite and two poytypic modifications were found for gageite. The gageite 2M is monoclinic and isostructural with balangeroite, while gageite 1Tc is triclinic [87F1]. The analysis was carried out with reference to the C-centered cell characterized by translation periods $A = 2a$, $B = 2b$, $C = c$ ($2a \times 2b \times c$ cell). The structural topology of balangeroite and gageite 2M is represented in Fig. 4. The level of the tetrahedral chains is denoted by the height, in C/6 units, of the bridging oxygen atoms in both disilicate groups placed along [001] that build up the repeat unit of the chain. Both unit cells: the C-centered double cell with A and B translations, and the simple cell with a_m and b_m translation parameters are outlined. The symmetry elements are also shown in the latter cell: twofold axes, inversion centers at levels 0 and 3, in $c_m/6$ units, and n glides at levels 1.5 and 4.5, in $c_m/6$ units. The resulting space-group symmetry is P2/n, with the twofold axis in the ***c*** direction. In Fig. 4b the structural arrangement in gageite 1Tc is given. The heights of the

various tetrahedral chains are indicated, and the unit-cell translations a_t and b_t are outlined, both starting from the inversion center at level 2, in $c_t/6$ units, assumed as origin, and ending on inversion centers at level 4. The resulting space group is $P\bar{1}$. In Figs. 4(c-e) the schematic drawings are plotted where the composite T-**O-**T modules are represented by segments oriented as the projection of the octahedral walls, with the relative heights of the modules indicated. The structural schemes for both monoclinic and triclinic forms are compared with the hypothetical $a \times b \times c$ structure which is orthorhombic and has the space group symmetry Pnnm.

The polytypic relationship between the monoclinic and triclinic modifications may be conveniently treated in more formal terms acoording to the order-disordered (OD) theory [56D1, 72D1], which takes into account the equivalent layers (for OD theory see section "true micas", vol. 27I5). The monoclinic structural type in balangeroite and gageite 2M and the triclinic type in gageite 1Tc correspond to distinct ordered members of a whole OD-structure family that includes those structures in which all the pairs of adjacent layers are geometrically equivalent. The monoclinic and triclinic structural arrangements may be described as consisting of equivalent layers, characterized by translation periods a_m and c_m and width $b_o = b_m/2$. Adjacent layers are related by the vector $\boldsymbol{t}_1 = -\boldsymbol{a}_m/2 + \boldsymbol{b}_o + \boldsymbol{c}_m/3$ or the vector $\boldsymbol{t}_2 = -\boldsymbol{a}_m/2 + \boldsymbol{b}_o - \boldsymbol{c}_m/3$. Only two members exist with the maximum degree of order. These are members in which n-tuples ($n \geq 3$) are geometrically equivalent. They correspond to the layer sequence $\boldsymbol{t}_1\boldsymbol{t}_2\boldsymbol{t}_1\boldsymbol{t}_2$ ... which is realised in the monoclinic modifications, whereas the sequence $\boldsymbol{t}_1\boldsymbol{t}_1\boldsymbol{t}_1$ ... (or $\boldsymbol{t}_2\boldsymbol{t}_2\boldsymbol{t}_2$ ...) is realised in the triclinic modification. For crystal structure of balangeroite see also [91B1].

The first report of the crystal structure of *harstigite* discuss the relation between gageite and harstigite [68M1, 68M2]. The crystal structure of harstigite, $MnCa_6Be_4[SiO_4]_2[Si_2O_7]_2(OH)_2$ was determined later [86H1]. The silicate crystallizes in an orthorhombic-type lattice having space group Pnam. Harstigite is a mixed-anion silicate which contains $[SiO_4]$ tetrahedra, $[Si_2O_7]$ groups and in addition $[Be(O,OH)_4]$ tetrahedra, $[MnO_6]$ polyhedra and $[CaO_8]$ polyhedra. The ratio of the single tetrahedra $[SiO_4]$ to double tetrahedra $[Si_2O_7]$ in the structure is 1:1. The tetrahedra form four-membered, five-membered and eight-membered rings which, connected with one another, give rise to layers of composition $Be_8[(SiO_4]_4[(Si_2O_7)]_4(OH)_4$ parallel to (100). These layers are held together by the Ca and Mn ions which occur between them. Three of the oxygen atoms that form the Be2 and Be3 tetrahedra are shared with Si tetrahedra and two OH groups labelled O14 and O15 complete the Be tetrahedra. The presence of OH groups at these locations shows up from a difference Fourier synthesis and a valence bond analysis [85B1].

Johninnesite

Johninnesite, having the ideal composition $Na_2Mg_4Mn_{12}As_2Si_{12}O_{43}(OH)_6$ crystallizes in a triclinic-type lattice having space group P1 or $P\bar{1}$ [86D1].

Pumpellyite, julgodite, okhotskite, shuiskite

Pumpellyites are mixed group silicates containing isolated $[SiO_4]$ tetrahedra and disilicate $[Si_2O_6(OH)]$ groups. The general formula is commonly indicated as $W_8X_4Y_8Z_{12}O_{56-n}(OH)_n$ where W are sevenfold-coordinated sites commonly occupied by Ca, X and Y are two crystallographically independent octahedral sites occupied by divalent and trivalent cations, and Z indicates tetrahedral sites invariably occupied by Si [73P1]. Structure analogous chemical variants of pumpellyite are the minerals *julgoldite*, [71M1, 73A1], *shuiskite* [81I1, 82F1], *okhotskite* [87T1] and *V-pumpellyite* [92P1]. The mineral is to be named pumpellyite, julgoldite, shuiskite or okhotskite, where Al, Fe, Cr or Mn, respectively, is the prevailing cation in the Y-octahedral site [73P1]. A suffix can be added to denote the dominant cation in the X octahedral site. The structure and crystal chemistry of pumpellyites are closely related to a number of minerals containing disilicate (sursassite, macfallite) or trisilicate groups (ardennite, orientite). All these silicates can be considered polytypes on the basis of the order-disorder (OD) theory, because their ideal OD-structures can be derived from two different kinds of layer unit stacked in regular alternation [91P1].

The crystal structure of Ca-containing pumpellyites were analysed in the space group A2/m. The structure contains octahedra which share edges to form infinite linear chains parallel to the [010] direction. There are two symmetrically independent chains, one of which is composed of the M2 octahedra on a special position, while the other is formed by M1 octahedra on the general position. The M2 site has a higher symmetry of the two

octahedral sites. In the unit cell, there are four symmetrically equivalent M2 sites, and eight M1 sites, therefore four M1 chains and two M2 chains run parallel to [010]. The shared edges in the chains are O9 - O11 for the M2 site and O5 - O6 and O4 - O7 for the M1 site. The existence of both double tetrahedra $Si_2O_6(OH)$ and isolated tetrahedra SiO_4 is characteristic for the structure. There is no edge shared between the tetrahedra and octahedra. Tetrahedra which alternate at heights y = 0.0 and 0.5 laterally bridge between O1 - O1, O2 - O2 and O3 - O3 vertices (unshared edges) of different octahedra. The cross-linking by octahedra and the tetrahedra exists as shown in Fig. 5 [85Y1]. The octahedra-tetrahedra linkage therefore results in a three-dimensional framework. This framework is sufficiently open to accommodate a calcium atom. The coordination polyhedron of seven oxygen atoms around each calcium atom is described as a square with two oxygen atoms on one side and one on the other. Ca1 polyhedra share the edges O3 - O4 with M1-octahedra and edges O2 - O11 with M2 octahedra, and the Ca2-polyhedra also share the edges O1 - O6 with M1-octahedra and the edges O2 - O9 with M2 octahedra. Ca1 and Ca2 polyhedra share the edges O1 - O8 with Si1-tetrahedra and the edges O6 - O9 with Si3-tetrahedra, respectively.

Most of the structural studies concerning pumpellyite-type silicates have been performed by single crystal X-ray diffraction on Al-rich [65G1, 69G1, 71A1, 71B1, 85Y1] and Fe-rich end members [71M1, 73A1]. Several studies revised the crystal chemical role of iron in pumpellyite-type structure by means of X-ray powder Rietveld refinement, X-ray absorption spectroscopy and ^{57}Fe NGR data [91A1, 94A1, 95A1]. These studies showed that iron is mostly trivalent and that Fe^{2+} and Fe^{3+} are distinct over the two crystallographically independent octahedral sites, with Fe^{3+} located at the smaller and more distorted Y site and Fe^{2+} located on the larger and more regular X-site.

Since pumpellyites, from low-grade metamorphic rocks, often contain a substantial amount of Mn, the silicates are better described in the Al-end-member pumpellyite – Fe-end member julgoldite – Mn-end member okhotskite compositional projection [91D1]. In [87T1, 96A1] was shown that Mn in pumpellyite is distributed over both octahedral sites. Mn^{2+} is prevalent in the more symmetrical octahedral X site, and Mn^{3+} is prevalent in the octahedral Y site. This is in agreement with the ionic size difference between the two octahedrally coordinated cations and with the partitioning of Fe^{2+} and Fe^{3+} in Fe-rich pumpellyite minerals [94A1].

The vanadium rich silicates (1.7 to 13.6 wt % V_2O_3) of the pumpellyite group were studied [92P1]. In addition to a substantial amount of V, these are characterized by unusually high As, Mg and F contents. Vanadium is incorporated into the pumpellyite structure mainly by direct substitution $Al^{3+} \leftrightarrow V^{3+}$, with minor contributions from $2Al^{3+} \leftrightarrow V^{4+} + (Mg, Fe)^{2+}$ or $3Al^{3+} \leftrightarrow V^{5+} + 2(Mg, Fe)^{2+}$ or both. In vanadium pumpellyite-(Mg), As seems to substitute for Si in tetrahedral positions [92P1].

Ca-free pumpellyite, $Mg_5Al_5Si_6O_{21}(OH)_7$, was synthesized from a gel composition $5MgO{\cdot}2.5Al_2O_3{\cdot}6SiO_2$ in the presence of excess H_2O [86S1, 87S1]. This silicate was identified as analogue of pumpellyite [80S1] and labeled as (Mg,Al) pumpellyite. According to [86S1, 87S1, 91P1, 99A1], for $Mg_8(Mg_2Al_2)Al_8Si_{12}(O,OH)_{56}$ composition, the name MgMgAl-pumpellyite was proposed, which indicates the presence of Mg in W site. This phase was shown to be stable above 3.4 GPa and at temperatures up to 820ºC. It was recognized as a water carrier in mantle [98F1]. Later on, it was shown that this silicate is isostructural with sursassite and has been called Mg-sursassite [00G1]. The crystal structure was presented in section 8.1.2.7 together with that of sursassites. For pumpellyite solid solution see also [84M1, 96C1, 97A1].

Rustamite

Rustamite, $Ca_{10}(Si_2O_7)_2(SiO_4)(OH)_2Cl_2$, crystallizes in a monoclinic lattice having Cc or C2/c space group [65A1].

Rosenhahnite, thalenite, jennite

The hydrous calcium silicate *rosenhahnite*, $Ca_3Si_3O_8(OH)_2$, was first described by [67P1] who proposed the chemical formula $(CaSiO_3)_3{\cdot}H_2O$. They showed that the complete dehydration of rosenhahnite crystals at 420…540ºC, result in single crystals of β-$CaSiO_3$ (wollastonite), which maintain a perfect topotactic relation to the parent silicate. In [73J1] was noted that the structure of rosenhahnite contains $Si_3O_8(OH)_2$ groups and the chemical formula should be written as $Ca_3Si_3O_8(OH)_2$. They further showed that the trisilicate groups are arranged as hydrogen-bonded linear chains in the structure and the dehydration involves joining of these

trisilicate groups in chains by splitting out water molecules. A full description of the structure was reported by [77W1]. This consists of three crystallographically independent Ca-polyhedra, $Ca1O_7$, $Ca2O_7$ and $Ca3O_7$ and a hydroxylated trisilicate group $[Si_3O_8(OH)_2]$ - Fig. 6 [77W1].The trisilicate group with point symmetry 1 consists of a central SiO_4 tetrahedron sharing corners with two adjancent $SiO_3(OH)$ tetrahedra.The trisilicate group exhibits point symmetry 1 as in thalenite $Y_3(Si_3O_{10})(OH)$ [72K1].The electronegativity difference between the bonded atoms indicates that the bonding within the trisilicate group in rosenhahnite is considerably more covalent than that between oxygen atoms of the group and the Ca ions. A similar situation is expected in thalenite. In both structures, the non-tetrahedral cations are asymmetrically distributed around the trisilicate ion. As a result the ion is distorted from ideal mm2 conformation to satisfy the packing and bonding requirements of both the non-tetrahedral cations and the trisilicate ion. This distortion affects both the Si–O bond lenghts and O–Si–O and Si–O–Si valence angles. One hydrogen atom bonds the trisilicate groups in linear chains, and the other links adjacent trisilicate groups across symmetry centers into a three-dimensional array. The lack of symmetry in the trisilicate group, along with significant differences in the dimensions of the three silicate tetrahedra, was attributed to electrostatic interactions between the nonbridging oxygen atoms and Ca^{2+} ions, which are asymmetrically distributed around the trisilicate group.

The structure of *thalenite*, $Y_3[Si_3O_{10}](OH)$, has been determined by [72K1]. Later on, thalenite containing 3.39 % of fluorine was reported [85V1]. The composition of thalenite with extensive substitution of Y by R elements was analysed. Upon heating, even at moderate temperatures, both the crystalline and the metamict thalenite are converted to a phase with a structure corresponding to that of thortveitite, $Y_2Si_2O_7$ [86F1]. The metamict character is caused by the radiation from uranium and thorium, present as impurities in structure. The thalenite crystallizes in a monoclinic structure having space group $P2_1/n$ [88Y1]. The Y^{3+} cations, in three independent positions in the structure, lie in seven-pointed polyhedra, which are distorted octahedra with a pyramid on one of the faces (Y1), a distorted trigonal prism with a semioctahedron on the side face (Y2) and eight-pointed polyhedron (Y3). The structure of thalenite is a three-dimensional crystalline assemblage of large Y polyhedra, joined by common vertices of edge - Fig. 7 [88Y1]. The common edges of the polyhedra are regularly shortened. Along the ***a***-axis of the structure there are columns joined by common edges of Y2 polyhedra. In turn, each of the seven-pointed Y2 polyhedra has an edge link with two Y1 seven-pointed polyhedra. The latter are also joined via common edges each to two Y3 eight-pointed polyhedra. Joined by vertices, the Y2 and Y3 polyhedra complete the formation of a framework of large Y^{3+} cations. The “flexible” groups of three silicon tetrahedra $[Si_3O_{10}]$ impart additional rigidity to the framework by joining the vertices and edges of the Si tetrahedra with the Y polyhedra. Each Si3 tetrahedron has two common edges with the Y2 and Y3 polyhedra, and the Si2 tetrahedron has a common edge with the eight-pointed Y3 polyhedron. The Si1 tetrahedra are joined to the Y polyhedra only by vertices [88Y1].

In the original description of *jennite*, [66C1] reported the composition $Na_2Ca_8Si_5O_{30}H_{22}$. Later on, [77G1] showed that composition approximates to $9CaO{\cdot}6SiO_2{\cdot}11H_2O$ with the possible ionic constitution $Ca_9Si_6O_{16}(OH)_{10}{\cdot}6H_2O$. The dehydration product called *metajennite* has the composition $Ca_9Si_6O_{16}(OH)_{10}{\cdot}2H_2O$. The structure of jennite, $Ca_9Si_6O_{16}(OH)_{10}{\cdot}6H_2O$ can be described in terms of main layers and interlayers which leads to the above constituent formula [66C1, 77G1]. The main layer appears to be a sandwich, in which a central Ca–O part is flanked on each side by parallel rows of Si_3O_9H chains. Only one half of the O atoms of the central part is shared with the chains, the other being part of OH groups. The combined thickness of the main layer and interlayer is 10.5 Å. On heating at 110ºC or drying at 23ºC and a vapor pressure of 66 mPa, four molecules of H_2O are lost and metajennite is formed. This has a layer thickness of 8.7 Å. The XRD study evidences that the central Ca–O parts of the main layers are related to the simple octahedral layers that exist in $Ca(OH)_2$ [86T1]. In jennite, the silicate chains are, in theory, infinitely long, and kinked so as to repeat at intervals of three tetrahedra - Fig. 8. In each group of three tetrahedra, two share O atoms with the central Ca–O part of the layer; the third, which does not, was called a “bridging” tetrahedron [86T1]. If some or all of these bridging tetrahedra were missing, finite chains containing 2, 5, 8, ..., 3n-1 tetrahedra would result. There appears to be one H atom attached to each bridging tetrahedron - Fig. 8A. It was assumed [86T1] that, when a bridging tetrahedron is omitted, one of the broken ends of the chain carries a H atom and the other does not - Fig. 8B. This leaves the net charge unchanged and thus implies that omission of tetrahedron does not require any change in the amount of interlayer Ca [86T1]. We note that jennite has been synthesized by reactions in aqueous suspensions at 60ºC to 80ºC [80H1].

8.1.2.8.2 Nuclear gamma resonance (NGR) data

Balangeroite

The ^{57}Fe NGR spectra of balangeroite were analysed considering the presence of two Fe^{2+} and two Fe^{3+} doublets, both at 80 K and 293 K [94D1] - Fig. 9. The hyperfine parameters for the Fe^{2+} doublets are typical for octahedral coordination. The δ values for Fe^{3+} are unusually large for octahedral coordination. Most iron is in ferrous state (≅ 80 %). The present data suggest two families of octahedra. Since in the monoclinic cell each "independent" octahedron of the orthorhombic subcell is splitted in six independent, but presumably very similar octahedra, a substantial broadening of the lines arises. The large differences between quadrupole splittings, ΔQ, show that the octahedra are differently distorted in agreement with structure analysis (see section 8.1.2.8.1). The Fe^{3+} content (20 %) is smaller than the value of 32 % determined by X-ray analysis [83C1]. A reason for the difference can be the uncertainty level arising from the presence of unresolved ^{57}Fe NGR lines [75D1]. - See also Table 5.

Pumpellyite

According to [97C1, 97C2], the ^{57}Fe NGR spectra were decomposed in three subspectra. The values of isomer shifts (δ) and quadrupole splittings (ΔQ) in both spectra suggest the presence of ferrous ions in the sixfold-coordinated sites for the first doublet and ferric ones for the second and third doublets - Fig. 10 [97C2]. In order to attribute the two Fe^{3+} doublets to X and Y sites, the authors performed a numerical computation of the lattice and ionic contributions to the electric field field gradient, by using the point charge model. We note that the calculated ΔQ values [Fe^{2+}: ΔQ(X) = 2.68(8) mm/s; Fe^{3+}: ΔQ(X) = 0.86(8) mm/s; ΔQ(Y) = 1.91(10) mm/s] are close to those experimentally determined - Table 5.

The ^{57}Fe NGR study of other pumpellyites [94A1] show that the spectra can be described in their simplest form as a three-peak envelope. Finally, the authors considered a simple two-doublets fit although this does not appear to be strictly correct. These authors suggest that the Fe^{2+} and Fe^{3+} content assigned to the X and Y sites are not sensibly different from the values obtained by a more complex fit, as evidenced by comparing with the results of Rietveld analysis - Table 5. By using ^{57}Fe NGR study and X-ray diffraction, it has been concluded that: (1) Al is the prevalent species both in X and Y sites (true pumpellyite - (Al)); (2) the crystallographic Y-site appears to be occupied by iron, primarily in Fe^{3+} state, and the ratio Fe/Al of this site is proportional to the total iron content; (3) the crystallographic X-site contains up to 30 % Fe^{2+} and this occupancy is not proportional to the total Fe content; (4) Fe cations with different valence states appear to be partioned into the two different octahedral sites with Fe^{2+} favouring the larger and more symmetrical X-position. This site preference is in agreement with the proposed general substitution scheme $MgAl \Leftrightarrow Fe^{2+}Fe^{3+}$ between ideal pumpellyite and julgoldite end members [71M1, 81O1, 85D1]. The samples from low grade metamorphic rocks contain a majority of iron in the Fe^{3+} state.

Okhotskite

The room temperature ^{57}Fe NGR spectrum consists of three doublets [87T1]. One doublet is identified as belonging to Fe^{3+} in the M3 site of piemontite [67B1, 73D1]. The remaining two doublets were identified as belonging to Fe^{3+} in okhotskite[34)] - Table 5.

8.1.2.8.3 Nuclear magnetic resonance (NMR) data

Zunyite

Zunyite has been studied by means of ^{27}Al NMR [84K1, 95D1]. The ^{27}Al MAS-NMR spectrum is shown in Fig. 11a [95D1]. The data obtained from the analysis of the spectrum are listed in Table 6. The 71.4-ppm signal is due to Al from the central AlO_4 tetrahedron; the 7.7 ppm signal with the highest intensity represents Al from the 12 AlO_6 octahedra around the AlO_4 group [95D1]. There are also signals at 46.6 ppm and –3.4 ppm. The 46.6 ppm peak (B_0=14.1 T) shifts to 46.1 and 46.3 ppm at magnetic fields of 7.1 and 11.7 T, respectively. This corresponds to an isotropic chemical shift of 46.8 (5) ppm and a QCC = 0.5…1.0 MHz. This was attributed to the excess of Al incorporated into the Si_3O_{16} pentamer. The –3.4-ppm signal was caused by an impurity.

^{29}Si MAS NMR spectra in zunyite were reported by [83G1, 91S1, 95D1]. A typical spectrum is plotted in Fig. 11b [95D1]. As mentioned in section 8.1.2.8.1 - Fig. 1, the Si_5O_{16} pentamer consists of a central Q^4(4Si) Si atom and four Q^1(1Si) Si atoms with Si–O–Si intertetrahedral angles of 180° - Fig. 1. The -96.6 ppm peak was attributed to Si in a Q^1(1Si) configuration with Si–O–Si angles of 180°. The –128.2 ppm peak is due to Si in a Q^4(4Si) configuration, also with Si–O–Si angles of 180°. The relative intensities of the Q^1(1Si) and Q^4(4Si) are 1:4, as expected from the stoichiometry of the pentamer. The –91.2 ppm peak was assumed to arise from nacrite ($Al_2Si_2O_5(OH)_4$) present as an impurity [83G1, 91S1]. In [95D1] a kaolinite was reported as a secondary phase, but this is closely related to nacrite. In [95D1] was noted that the value –91.2 ppm is to be expected from a Si atom in a Q^1(1Al) site with Si–O–Al angles of 180°. This site is formed by incorporating Al into the Si1 site.

8.1.2.8.4 Optical properties

Davreuxite

The infrared spectrum of davreuxite[4)] is shown in Fig. 12 [84F1]. The main features determined from the spectrum are: (1) the presence of OH groups whose stretching vibrations form an intense doublet at 3396 and 3478 cm^{-1}, indicating by these frequencies the presence of hydrogen bonds; (2) determination of tetrahedral aluminium by the existence of the very intense band at 815 cm^{-1}; (3) occurrence of almost linear, strong Si–O–Al bonds in the structure, also indicated by the very intense band at 1200 cm^{-1}.

The refractive indices of some silicates, from groups mentioned in Table 1, are given in Table 7.

Tables and figures

Table 1. Silicate minerals from groups VIIIB20 – VIIIB28 [91N1].

Silicate	Ideal composition	Group
Zunyite	$Al_{13}Si_5O_{20}(OH,F)_{18}Cl$	VIIIB20
Davreuxite	$MnAl_6Si_4O_{17}(OH)_2$	VIIIB21
Keldyshite	$NaZrSi_2O_6(OH)$	VIIIB22
Parakeldyshite	$Na_2ZrSi_2O_7$	VIIIB22
Khibinskite	$K_2ZrSi_2O_7$	VIIIB22
Medaite	$(Mn,Ca)_6(V,As)Si_5O_{18}(OH)$	VIIIB23
Tiragalloite	$Mn_4AsSi_3O_{12}(OH)$	VIIIB23
Gageite-2M	$Mn_{21}O_3(Si_4O_{12})_2(OH)_{20}$	VIIIB24
Gageite-1Tc	$Mn_{21}O_3(Si_4O_{12})_2(OH)_{20}$	VIIIB24
Balangeroite	$(Mg,Fe)_{21}Si_8O_{27}(OH)_{20}$	VIIIB24
Harstigite	$Ca_6Be_4(Mn,Mg)Si_6O_{22}(OH)_2$	VIIIB24
Johninnesite	$Na_2Mg_4Mn_{12}As_2Si_{12}O_{43}(OH)_6$	VIIIB25
Pumpellyite-(Fe^{3+})	$Ca_2Fe^{3+}Al_2(SiO_4)(Si_2O_7)(OH,O)_2 \cdot H_2O$	VIIIB26
Pumpellyite-(Fe^{2+})	$Ca_2Fe^{2+}Al_2(SiO_4)(Si_2O_7)(OH)_2 \cdot H_2O$	VIIIB26
Pumpellyite-(Mg)	$Ca_2MgAl_2(SiO_4)(Si_2O_7)(OH)_2 \cdot H_2O$	VIIIB26
Pumpellyite-(Mn)	$Ca_2MnAl_2(SiO_4)(Si_2O_7)(OH)_2 \cdot H_2O$	VIIIB26
Shuiskite	$Ca_2MgCr_2(SiO_4)(Si_2O_7)(OH)_2 \cdot H_2O$	VIIIB26
Okhotskite	$Ca_2(Mn,Mg)(Mn,Al,Fe)_2Si_3O_{10}(OH)_4$	VIIIB26
Julgoldite-(Fe^{2+})	$(Ca,K)_2Fe^{2+}Fe^{3+}Si_3(O,OH)_{14}$	VIIIB26
Julgoldite-(Fe^{3+})	$(Ca,K)_2Fe^{3+}Fe^{3+}Si_3(O,OH)_{14}$	VIIIB26
Julgoldite-(Mg)	$(Ca,K)_2MgFe^{3+}Si_3(O,OH)_{14}$	VIIIB26
Rustamite	$Ca_{10}(Si_2O_7)_2(SiO_4)_4(OH)_2Cl_2$	VIIIB27
Rosenhahnite	$Ca_3Si_3O_8(OH)_2$	VIIIB28
Thalenite-(Y)	$Y_3Si_3O_{10}(OH)$	VIIIB28
Jennite	$Ca_9Si_6O_{16}(OH)_{10} \cdot 6H_2O$	VIIIB28

Table 2. Atomic sites and thermal parameters.

a) Zunyite[1)] having space group $F\bar{4}3m$ [82B1].

Atom	Equipoint	Point symmetry	x	y	z	$B_{eq} \cdot 10^2$ [Å^2]
Si1	4c	$\bar{4}3m$	1/4	1/4	1/4	31(1)
Si2	16e	3m	0.11430(2)	0.11430(2)	0.11430(2)	26(1)
Al1	4d	$\bar{4}3m$	3/4	3/4	3/4	25(1)
Al2	48h	m	0.08556(2)	0.08556(2)	0.76670(3)	35(1)
O1	16e	3m	0.82478(6)	0.82478(6)	0.82478(6)	35(1)
O2	16e	3m	0.18243(7)	0.18243(7)	0.18243(7)	89(2)
Oh3	24f	mm	0.27949(8)	0	0	66(2)
Oh4	48h	m	0.17870(4)	0.17870(4)	0.54601(6)	63(2)
O5	48h	m	0.13834(4)	0.13834(4)	0.00152(6)	44(1)
Cl	4b	$\bar{4}3m$	1/2	1/2	1/2	77(1)
H1a	48h	m	0.00228	0.00228	0.00530	1300
H1b	48h	m	0.00190	0.00190	0.00480	1300
H2	24f	mm	0.00336(3)	0	0	190

[1)] for composition see footnote in Table 4.

b) Davreuxite [6)] having monoclinic structure, space group $P2_1/m$ [84S1].

Atom	Site	x	y	z	$\beta_{ij} \cdot 10^3$ [a)]					
					β_{11}	β_{22}	β_{33}	β_{23}	β_{13}	β_{12}
Mn	2e	0.3516(2)	0.25	0.6351(1)	15(1)	4(1)	26(1)	0	3(1)	0
Si1	2e	0.8115(3)	0.25	0.4796(1)	9(1)	1(1)	13(1)	0	2(1)	0
Si2	2e	0.4962(3)	0.25	0.3911(2)	11(1)	2(1)	15(1)	0	4(1)	0
Si3	2e	0.6823(3)	0.25	0.0966(2)	8(1)	1(1)	14(1)	0	2(1)	0
Si4	2e	0.8992(3)	0.25	0.8574(2)	9(1)	3(1)	14(1)	0	2(1)	0
Al1	2e	0.3196(3)	0.25	0.9032(2)	10(1)	4(1)	15(1)	0	1(1)	0
Al2	2e	0.0906(3)	0.25	0.1340(2)	9(1)	2(1)	15(1)	0	1(1)	0
Al3	4f	0.9387(2)	0.9953(3)	0.3075(2)	10(1)	0(1)	13(1)	0(1)	3(1)	0(1)
Al4	4f	0.4026(2)	0.0008(3)	0.1547(2)	9(1)	1(1)	14(1)	1(1)	2(1)	0(1)
O1	2e	0.9844(7)	0.25	0.9915(6)	15(1)					
O2	2e	0.4742(6)	0.25	0.8548(5)	10(1)					
O3	2e	0.5279(6)	0.25	0.1268(5)	11(1)					
O4	2e	0.7230(6)	0.25	0.8375(5)	10(1)					
OH5	2e	0.3656(7)	0.25	0.4535(5)	12(1)					
O6	2e	0.6499(7)	0.25	0.4992(5)	11(1)					
O7	2e	0.2786(6)	0.25	0.1501(5)	10(1)					
O8	2e	0.8290(7)	0.25	0.2097(5)	12(1)					
O9	2e	0.9432(7)	0.25	0.6047(5)	11(1)					
OH10	2e	0.0555(6)	0.25	0.3790(5)	9(1)					
O11	2e	0.1720(6)	0.25	0.7733(5)	1(1)					
O12	4f	0.8248(4)	0.0158(7)	0.4084(3)	9(1)					
O13	4f	0.6829(4)	0.0144(7)	0.0223(3)	9(1)					
O14	4f	0.0593(4)	0.9850(7)	0.2017(3)	10(1)					
O15	4f	0.4906(4)	0.0209(7)	0.3141(4)	11(1)					

[6)] for composition see footnote in Table 4; [a)] The β_{ij} are defined by the expression for the temperature factor $T = \exp[-2\pi^2(\beta_{11}h^2a^{*2} + \ldots\ldots\beta_{12}hka^*b^*)]$.

Table 2 (continued)

c) Gageite[13] having orthorhombic-type substructure, space group Pnnm [87F1].

Atom	Composition	x	y	z	B_{eq} [Å^2]	Multiplicity
M1	0.36 Mn+0.64 Mg	0	0	1/2	0.66(5)	2.00
M2	0.46Mn+0.54Mg	0.3376(1)	0.3840(1)	1/2	0.76(4)	4.00
M3	1.00 Mn	0.4225(1)	0.1518(1)	0	0.99(3)	4.00
M4	1.00 Mn	0.1016(1)	0.4991(1)	0	0.82(3)	4.00
Si1		0.2109(2)	0.0967(2)	0.4568(15)	0.47(6)	2.67
Si2		0.0671(2)	0.1948(2)	0.0355(18)	0.54(6)	2.67
O1		1/2	0	0	1.02(10)	2.00
O2		0.3313(4)	0.0915(4)	1/2	1.11(8)	4.00
O3		0.3420(3)	0.2845(4)	1/2	1.05(8)	4.00
O4		0.4918(3)	0.3988(3)	1/2	1.07(7)	4.00
O5		0.3489(4)	0.4917(4)	1/2	1.22(8)	4.00
O6		0.1878(3)	0.3904(3)	1/2	0.84(7)	4.00
O7		0.0201(4)	0.3056(4)	1/2	1.17(7)	4.00
O8		0.1922(10)	0.1425(10)	0	0.98(20)	1.33
O9		0.1640(6)	0.1823(6)	0.7479(29)	0.53(13)	2.67
O10		0.1136(11)	0.1919(10)	1/2	0.73(20)	1.33

[13] for composition see footnote in Table 4.

d) Harstigite[19] having orthorhombic-type structure, space group Pnam [86H1].

Atom	x	y	z	$\beta_{ij} \cdot 10^4$					
				β_{11}	β_{22}	β_{33}	β_{23}	β_{13}	β_{12}
Mn	0.9993(1)	0.3950(1)	0.2500	76(3)	81(3)	164(3)	0	0	–1(3)
Ca1	0.9962(1)	0.6083(0)	0.3859(1)	66(2)	76(2)	93(2)	–13(2)	–12(2)	–4(2)
Ca2	0.5086(1)	0.3157(0)	0.3876(1)	60(2)	94(2)	85(2)	–20(2)	6(2)	12(2)
Ca3	0.5004(1)	0.5897(0)	0.3926(0)	66(2)	74(2)	85(2)	–7(2)	–26(2)	16(2)
Si1	0.2281(1)	0.2579(1)	0.2500	39(5)	45(5)	83(5)	0	0	–1(4)
Si2	0.2831(1)	0.5151(1)	0.2500	20(4)	55(5)	45(4)	0	0	–1(4)
Si3	0.2142(1)	0.5498(1)	0.5490(1)	47(3)	39(3)	73(4)	12(3)	6(3)	9(3)
Si4	0.2325(1)	0.7485(1)	0.4521(1)	35(3)	47(3)	74(3)	–3(3)	10(3)	2(3)
Be1	0.2381(5)	0.4017(4)	0.4159(3)	95(18)	79(16)	72(16)	12(15)	–9(14)	21(15)
Be2	0.2624(7)	0.5394(5)	0.7500	26(23)	70(24)	192(31)	0	0	15(20)
Be3	0.2657(7)	0.7284(4)	0.2500	78(24)	50(22)	1(18)	0	0	2(18)
O1	0.1579(3)	0.6590(2)	0.5144(2)	63(9)	67(10)	128(11)	31(8)	11(8)	8(8)
O2	0.3952(2)	0.7417(2)	0.4549(2)	44(8)	71(9)	124(10)	14(8)	–5(8)	–8(8)
O3	0.1701(2)	0.8459(2)	0.5036(2)	54(9)	84(10)	92(10)	–28(8)	17(8)	–2(8)
O4	0.1675(3)	0.7400(2)	0.3458(2)	64(9)	133(11)	55(8)	–13(8)	5(7)	–29(8)
O5	0.1373(3)	0.4746(2)	0.4765(2)	68(9)	55(9)	81(9)	–51(8)	–11(8)	3(7)
O6	0.1529(2)	0.5308(2)	0.6577(2)	31(9)	91(10)	113(10)	4(8)	–2(8)	0(7)
O7	0.3778(2)	0.5504(2)	0.5471(2)	46(9)	61(9)	90(9)	–4(7)	4(7)	6(8)
O8	0.1602(3)	0.3165(2)	0.3434(2)	92(9)	40(8)	65(8)	–11(7)	–3(8)	–11(7)
O9	0.3425(3)	0.4606(2)	0.3460(2)	75(9)	38(8)	75(9)	10(7)	–21(7)	–13(7)
O10	0.1172(4)	0.5239(3)	0.2500	25(12)	137(15)	93(13)	0	0	–14(12)
O11	0.1590(4)	0.1485(3)	0.2500	52(13)	66(13)	109(14)	0	0	51(11)

Table 2 (continued)

Atom	*x*	*y*	*z*	$\beta_{ij} \cdot 10^4$					
				β_{11}	β_{22}	β_{33}	β_{23}	β_{13}	β_{12}
O12	0.3926(3)	0.2476(3)	0.2500	43(12)	64(12)	87(12)	0	0	35(11)
O13	0.3507(3)	0.6245(3)	0.2500	15(11)	64(12)	120(14)	0	0	16(10)
O14	o.3666(4)	0.4499(3)	0.7500	111(15)	86(13)	69(13)	0	0	9(12)
O15	0.1115(5)	0.3146(30	0.7500	105(16)	72(14)	176(17)	0	0	75(13)
H1	0.176(12)	0.883(8)	0.250	810(41)					

[18] for composition see footnote in Table 4.

e) Pumpellyite[24] having monoclinic structure, space group A2/m [85Y1].

Atom	*x*	*y*	*z*	$\beta_{ij} \cdot 10^5$					
				β_{11}	β_{22}	β_{33}	β_{12}	β_{13}	β_{23}
Ca1	0.25033(8)	0.5	0.33962(4)	221(9)	591(21)	31(2)	0.0	28(3)	0.0
Ca2	0.19044(9)	0.5	0.15453(4)	558(11)	380(20)	34(2)	0.0	–9.3	0.0
M1[a]	0.25469(8)	0.24585(13)	0.49589(4)	165(9)	315(21)	33(2)	8(10)	22(3)	–4(4)
M2[b]	0.5	0.25	0.25	289(11)	479(25)	55(2)	12(12)	32(3)	4(6)
Si1	0.05055(10)	0.0	0.08966(5)	150(10)	418(23)	34(2)	0.0	11(4)	0.0
Si2	0.16539(11)	0.0	0.24764(5)	209(10)	401(24)	38(2)	0.0	–3(4)	0.0
Si3	0.46524(10)	0.0	0.40323(5)	156(10)	432(23)	29(2)	0.0	16(4)	0.0
O1	0.13767(18)	0.22615(30)	0.07086(8)	253(18)	450(43)	55(4)	–44(24)	38(7)	2(11)
O2	0.26532(20)	0.23090(31)	0.24597(9)	381(20)	498(44)	59(4)	–15(25)	–4(7)	8(12)
O3	0.36694(19)	0.22415(33)	0.41795(9)	283(19)	522(44)	56(4)	112(25)	51(7)	13(11)
O4	0.13068(27)	0.5	0.44515(13)	201(26)	500(61)	53(6)	0.0	5(10)	0.0
O5	0.13328(30)	0.5	0.45815(15)	193(28)	596(65)	65(6)	0.0	9(11)	0.0
O6	0.36919(27)	0.5	0.04487(13)	205(27)	453(60)	53(6)	0.0	–10(10)	0.0
O7	0.36712(29)	0.0	0.03267(13)	179(28)	610(66)	71(6)	0.0	–4(11)	0.0
O8	0.03611(28)	0.0	0.17546(12)	203(27)	1072(72)	29(6)	0.0	6(10)	0.0
O9	0.47856(28)	0.5	0.17585(13)	242(28)	1330(79)	48(6)	0.0	33(10)	0.0
O10	0.06645(33)	0.0	0.31367(14)	354(32)	1772(92)	53(6)	0.0	22(11)	0.0
O11	0.50216(30)	0.5	0.31488(14)	281(30)	1128(75)	57(6)	0.0	40(11)	0.0
H5	0.069(17)	0.0	0.466(8)		B_{eq} [Å^2]	1.1(3.0)			
H7	0.444(7)	0.0	0.045(3)			0.3(1.4)			
H10	0.092(13)	0.0	0.343(6)			5.4(4.4)			
H11	0.443(9)	0.0	0.155(4)			3.0(2.2)			

[a] 1.00 Al ;
[b] 0.80Al + 0.20Fe;
[24] for composition see footnote in Table 4.

Table 2 (continued)

f) Rosenhahnite[39], $Ca_3Si_3O_8(OH)_2$, having space group $P\bar{1}$ [77W1].

Atom	*x*	*y*	*z*	B_{eq} [Å^2]
Ca1	0.27993(6)	0.34503(5)	0.18405(7)	0.669(7)
Ca2	0.09599(6)	0.68010(5)	0.24285(7)	0.643(7)
Ca3	0.84648(6)	0.00858(5)	0.26704(7)	0.698(7)
Si1	0.30412(8)	0.04876(7)	0.27718(9)	0.494(9)
Si2	0.62432(8)	0.66151(7)	0.32901(9)	0.482(9)
Si3	0.80203(8)	0.37614(7)	0.27028(9)	0.506(9)
O1	0.1928(2)	0.0874(2)	0.0902(3)	0.83(2)
O2	0.5003(2)	0.9696(2)	0.2131(3)	0.99(3)
O3	0.1594(2)	0.9480(2)	0.3668(3)	0.75(2)
O4	0.3938(2)	0.2132(2)	0.4471(3)	0.80(2)
O5	0.7694(2)	0.7254(2)	0.1969(3)	0.68(2)
O6	0.4085(2)	0.5931(2)	0.2071(2)	0.67(2)
O7	0.7211(2)	0.5330(2)	0.4128(2)	0.71(2)
O8	0.6082(2)	0.2950(2)	0.0911(3)	0.82(2)
O9	0.8560(2)	0.2716(2)	0.4015(3)	0.79(2)
O10	0.9748(2)	0.4193(2)	0.1475(3)	0.73(2)
H1	0.524(2)	0.101(6)	–0.122(8)	3.0(1.3)
H2	0.602(1)	0.342(4)	–0.020(6)	0.8(8)

[39] for composition see footnote in Table 4.

g) Thalenite[40] having monoclinic structure, space group $P2_1/n$ [88Y1].

Atom	*x*	*y*	*z*	B_{eq} [Å^2]
Y1	0.90512(9)	0.22965(6)	0.31144(6)	0.30(1)
Y2	0.23710(9)	0.53235(6)	–0.01781(6)	0.34(1)
Y3	0.30073(9)	0.40225(6)	0.49650(6)	0.50(1)
Si1	0.2325(3)	0.2453(2)	0.1112(2)	0.72(5)
Si2	0.4941(3)	0.0383(2)	0.2080(2)	0.72(5)
Si3	0.0231(3)	0.0861(2)	0.7408(2)	0.70(5)
O1	0.2698(7)	0.3192(4)	0.9832(4)	1.0(1)
O2	0.0164(7)	0.2286(5)	0.1211(4)	1.0(1)
O3	0.4662(7)	0.0226(5)	0.3611(4)	1.3(1)
O4	0.3193(7)	0.1089(4)	0.1231(4)	1.1(1)
O5	0.3434(7)	0.3238(5)	0.2313(4)	1.2(1)
O6	0.0244(7)	0.4121(4)	0.3710(4)	1.0(1)
O7	0.0128(7)	0.0243(5)	0.3611(4)	1.0(1)
O8	0.1864(7)	0.3941(4)	0.6922(4)	1.1(1)
O9	0.2075(7)	0.1440(5)	0.6974(4)	1.2(1)
O10	0.0403(7)	0.0506(4)	0.8919(4)	1.1(1)
F	0.1943(6)	0.2162(4)	0.4403(4)	1.5(1)

[40] for composition see footnote in Table 4.

Table 3. Geometric units in zunyite [82B1].

Composition	Description
$Al2_3O5_3Oh3_3O1Oh4_6$	Trimeric unit of the octahedra sharing corner O1 and edges O1-O5
$Al2_{12}O5_{12}Oh3_6O1_4Oh4_{24}$	Cluster around A formed by four trimeric units sharing corners Oh3
$Al2_{12}O5_{12}Oh3_6O1_4Oh4_{12}$	Octahedral framework formed by clusters A sharing corners Oh4
$Si1O2_4Si2_4O5_{12}$	Pentameric unit C of five SiO_4 tetrahedra surrounded tetrahedrally by A clusters with which it shares corners O5
$ClH2_6Oh3_6$	Octahedral B unit of hydrogen-bonded Cl surrounded octahedrally by six A units with which it shares corners Oh3
$Al1O1_4$	Tetrahedral D unit AlO4 surrounded tetrahedrally by four A units with which it shares corners O1
$Al1O1_4Oh4_{12}Al2_{12}O5_{12}Oh3_{12}$	Cuboctahedral cluster around D including central tetrahedron and four trimeric units sharing corners Oh4 with each other
$Al1O1_4O5_{12}Al2_{12}Oh4_{12}Oh3_6$	Framework formed by cuboctahedral clusters sharing corners Oh3

Table 4. Crystal structures and lattice parameters at RT.

Silicate	Space group	Lattice parameters				Refs.
		a [Å]	*b* [Å]	*c* [Å]	α, β, γ	
Zunyite[1)]	$F\bar{4}3m$	13.8654(5)				82B1
Zunyite[2)]	$F\bar{4}3m$	13.8796(3)				82B1
Davreuxite[3)]	monoclinic	9.57	5.79	12.88	$\beta = 116°$	76F1
Davreuxite[4)]	$P2_1/m$	9.550(2)	5.767(1)	12.077(2)	$\beta = 108°1(1)'$	84F1
Davreuxite[5)]	$P2_1/m$	9.556(3)	5.763(2)	12.084(4)	$\beta = 108°34(1)'$	84F1
Davreuxite[6)]	$P2_1/m$	9.518(6)	5.753(2)	12.04(1)	$\beta = 108°00(5)°$	84S1
Keldyshite[7)]	$P\bar{1}$	6.66	8.83	5.42	$\alpha = 92°45'$ $\beta = 94°13'$ $\gamma = 72°20'$	69K1
Parakeldyshite[7)]	P1	6.66	8.83	5.42	$\alpha = 92°45'$ $\beta = 94°15'$ $\gamma = 77°20'$	73K1
Parakeldyshite[8)]	$P\bar{1}$	5.419	6.607	8.806	$\alpha = 71°50'$ $\beta = 87.15°$ $\gamma = 85.63°$	77R1
Khibinskite[9)]	monocl. or triclinic	19.22	11.10	14.10	$\alpha = 90°$ $\beta = 116°30'$ $\gamma = 90°$	73K1
Medaite[10)]	$P2_1/n$	6.712(1)	28.948(8)	7.578(2)	$\beta = 95.40(2)°$	81G1, 82G1
Tiragalloite[11)]	$P2_1/n$	6.66(1)	19.92(2)	7.67(1)	$\beta = 95.7(1)°$	80G1
Gageite[12)]	Pnnm	13.79(2)	13.68(2)	3.279(3)		69M1
Gageite 2M[13)]	monoclinic	19.42	19.42	9.84	$\beta = 89.5°$	87F1
Gageite $1T_c$[13)]	triclinic	14.17	14.07	9.84	$\alpha = 76.5°$ $\beta = 76.6°$ $\gamma = 86.9°$	87F1

Table 4 (continued)

Silicate	Space group	Lattice parameters				Refs.
		a [Å]	*b* [Å]	*c* [Å]	α, β, γ	
Balangeroite[14)]	Pnnm	13.85(4)	13.58(3)	9.65(3)		83C1
Balangeroite[15)]	P2/n	19.163(2)	19.224(2)	9.599(3)	$\gamma = 89.50(1)°$	94D1
Balangeroite[16)]	monoclinic	19.40	19.40	9.65	$\gamma = 88.9°$	87F1
Balangeroite[17)]		19.163(2)	19.224(2)	9.599(3)	$\gamma = 89.50(1)°$	91B1
Harstigite[18)]	Pcmn	13.90	13.62	9.68		68M2
Harstigite[19)]	Pnam	9.793(2)	13.636(3)	13.830(3)		86H1
Johninnesite[20)]	P1 or $P\bar{1}$	10.44(2)	11.064(6)	9.62(1)	$\alpha = 107.43(7)°$ $\beta = 82.7(1)°$ $\gamma = 111.6(1)°$	86D1
Pumpellyite[21)]	$P2_1/m$	8.5759(4)	5.7295(2)	18.5376(9)	$\beta = 97.691(3)°$	99A1
Pumpellyite[22)]-(Mn)	A2/m	8.923	5.995	19.156	$\beta = 97°8'$	81K1
Pumpellyite[23)]	A2/m	8.83	5.90	19.17	$\beta = 97°7'$	69G1
Pumpellyite[24)]	A2/m	8.812(4)	5.895(2)	19.116(11)	$\beta = 97.41(7)°$	85Y1
Pumpellyite[25)]		8.8510(3)	5.9345(2)	19.1247(6)	$\beta = 96.969(1)°$	96A1
Pumpellyite[26)]		8.8330(4)	5.9153(3)	19.1009(8)	$\beta = 97.154(2)°$	96A1
Pumpellyite[27)]	A2/m	8.8193(2)	5.9042(2)	19.1138(5)	$\beta = 97.433(2)°$	94A1
Pumpellyite[28)]	A2/m	8.8192(2)	5.9192(3)	19.1274(5)	$\beta = 97.446(2)°$	94A1
Pumpellyite[29)]	A2/m	8.8375(2)	5.9520(2)	19.1812(5)	$\beta = 97.461(2)°$	94A1
Pumpellyite[30)]		8.82(3)	5.92(3)	19.11(4)	$\beta = 97.71(2)°$	92P1
Pumpellyite[31)]		8.82(4)	5.91(1)	19.15(2)	$\beta = 97.69(5)°$	92P1
Pumpellyite[32)]		8.83(1)	5.95(1)	19.15(3)	$\beta = 97.70(5)°$	92P1
Shuiskite[33)]	A2/m	8.897	5.843	19.41	$\beta = 98°$	81I1, 82F1
Okhotskite[34)]	A2/m	8.887(5)	6.000(4)	19.53(2)	$\beta = 97.08(6)°$	87T1
Julgoldite[35)]	A2/m	8.922(4)	6.081(3)	19.432(9)	$\beta = 97.60(6)°$	73A1
Julgoldite[36)]	A2/m	8.92(1)	6.09(1)	19.37(2)	$\beta = 97°30(5)'$	71M1
Rustamite[37)]	Cc or C2/c	7.62(5)	18.55(5)	15.51(5)	$\beta = 104°20(10)'$	65A1
Rosenhahnite[38)]	$P\bar{1}$ or P1	6.946(6)	9.474(6)	6.809(6)	$\alpha = 108°39'$ $\beta = 94°49'$ $\gamma = 95°43'$	67P1
Rosenhahnite[39)]	$P\bar{1}$	6.955(2)	9.484(2)	6.812(1)	$\alpha = 108.64(2)°$ $\beta = 94.84(2)°$ $\gamma = 95.89(2)°$	77W1
Thalenite-(Y)[40)]	$P2_1/n$	7.318(2)	11.134(8)	10.379(3)	$\beta = 97.24(2)°$	88Y1
Thalenite-(Y)[41)]		10.343	11.093	7.294	$\beta = 96°55'$	72K1
Thalenite-(Y)[42)]		10.38	11.16	7.319	$\beta = 97°14'$	86F1
Thalenite-(Y)[43)]		10.38	11.22	7.33	$\beta = 97°20'$	86F1
Jennite[50)]	triclinic	10.593	7.284	10.839	$\alpha = 99.67°$ $\beta = 97.65°$ $\gamma = 110.11°$	77G1
Metajennite[51)]	triclinic	10.590	7.278	9.511	$\alpha = 101.03°$ $\beta = 105.74°$ $\gamma = 110.10°$	77G1

Table 4 (continued)

[1] $Si_{4.95}Al_{13.05}O_{19.95}(OH)_{13.96}F_{4.09}Cl$;
[2] $Si_{4.68}Al_{13.32}O_{19.68}(OH)_{14.71}F_{3.61}Cl$;
[3] natural sample;
[4] $(Mn_{0.82}Mg_{0.07}Cu_{0.06}Zn_{0.04})(Al_{5.86}Fe^{3+}_{0.09})(Si_{4.01}P_{0.03})O_{17}(OH)_2$;
[5] $(Mn_{0.82}Mg_{0.12}Mg_{0.07})Al_{6.02}Si_{3.98}O_{17}(OH)_2$;
[6] $MnAl_6Si_4O_{17}(OH)_2$;
[7] natural sample;
[8] $Na_{1.89}(O(H_3O)_{0.054}K_{0.018}Ca_{0.015})(Zr_{0.990}Fe_{0.007}Ti_{0.005}Mg_{0.002})(Si_{1.987}Al_{0.012})O_{6.995}$, ideally, $Na_2ZrSi_2O_7$;
[9] no complete analysis (K_2O-23.5 %, Na_2O-1.8 %, CaO-0.9 %);
[10] $(Mn_{5.774}Ca_{0.190}Fe_{0.035})[(V_{0.815}As_{0.185})Si_5O_{18}(OH)]$;
[11] $(Mn_{3.909}Ca_{0.077}Fe_{0.013})[(As_{0.844}V_{0.116}Si_3O_{12}(OH)]$;
[12] $M^{2+}_7(O)(OH)_8[Si_2O_8]$ with M = Mn and Mg; substructure;
[13] $(Mg_{11.32}Fe_{0.11}Mn_{28.95}Ca_{0.14}Zn_{2.13})Si_{16}O_{54.53}(OH)_{40.23}$;
[14] $(Mg_{25.70}Fe^{2+}_{7.69}Fe^{3+}_{3.63}Mn^{2+}_{1.65}Al_{0.17}Ca_{0.07}Cr_{0.01}Ti_{0.01})Si_{15.38}O_{53.66}(OH)_{35.92}$;
[15] $(Mg_{0.62}Fe^{2+}_{0.19}Fe^{3+}_{0.10}Mn_{0.05}$ + minor content Al,Ca,Cr,Ti)$_{21}O_3(OH)_{20}(Si_4O_{12})_2$;
[16] $(Mg_{26.74}Fe^{2+}_{7.99}Fe^{3+}_{3.37}Mn_{1.71}Al_{0.18}Ca_{0.08}Cr_{0.01}Ti_{0.01})Si_{16}O_{55.81}(OH)_{37.35}$;
[17] $Mg_{14.52}Fe_{6.26}Mn_{0.19}Ca_{0.06}Al_{0.05}Cr_{0.03}Ti_{0.01}Si_8O_{37.17}$; the composition corresponds to the anhydrous residue of balangeroite. H_2O was not determined;
[18] $Mn_{0.86}Mg_{0.20}Ca_{5.88}Be_{4.00}Si_{5.80}O_{21.34}(OH)_{2.40}$;
[19] $MnCa_6Be_4[SiO_4]_2[Si_2O_7]_2(OH)_2$;
[20] $Na_{2.06}Mg_{4.20}Fe_{0.03}Mn_{11.83}As_{1.90}Si_{12.18}O_{43.22}(OH)_{5.95}$
[21] $Mg_8(Mg_2Al_2)Al_8Si_{12}(O,OH)_{56}$ This phase was later identified as Mg-sursassite;
[22] $(Ca_{7.54}Mn^{2+}_{0.39})(Mn^{2+}_{3.56}Mg_{0.46})(Al_{5.78}Mn^{3+}_{2.00}Fe^{3+}_{0.82})Si_{12.14}O_{41.62}(OH)_{13.04}$;
[23] $(Ca_{7.60}Mg_{0.40})(Mg_{1.20}Fe^{2+}_{0.77}Fe^{3+}_{0.18}Al_{10.00})[Si_{11.20}Al_{0.80}]O_{44}/\{(OH)_{9.29}(H_2O)_{2.71}\}$;
[24] $(Ca_{3.86}Na_{0.02}Mn_{0.08})Al_4(Al_{0.93}Fe_{0.46}Mg_{0.67})Si_{6.01}O_{21}(OH)_7$;
[25] $Ca_{8.12}(Al_{7.99}Mn_{3.41}Mg_{0.71}Fe_{0.30})Si_{11.84}O_{56-x}OH_x$;
[26] $Ca_{7.80}(Al_{8.91}Mn_{1.85}Mg_{1.16}Fe_{0.37})Si_{11.92}O_{56-x}OH_x$;
[27] $Ca_{7.61}Na_{0.20}Al_{10.80}Fe^{3+}_{0.26}Fe^{2+}_{0.51}Mg_{1.42}Si_{11.19}O_{56}(OH)_{14.79}$;
[28] $Ca_{7.39}Al_{8.88}Ti_{0.01}Fe^{3+}_{1.05}Fe^{2+}_{0.39}Mg_{1.50}Mn_{0.05}Si_{12.17}O_{56}(OH)_{14.83}$;
[29] $Ca_{7.41}Al_{7.27}Ti_{0.01}Na_{0.02}Fe^{3+}_{2.58}Fe^{2+}_{0.77}Mg_{1.29}Mn_{0.01}Si_{12.05}O_{56}(OH)_{15.25}$;
[30] vanadoan pumpellyite – (Mg) with 2.3 wt % V_2O_3;
[31] vanadoan pumpellyite – (Mg) with 4.6 wt % V_2O_3;
[32] vanadoan pumpellyite – (Mg) with 8.9 wt % V_2O_3;
[33] $(Ca_{3.82}K_{0.05}Na_{0.06})(Mg_{1.28}Fe_{0.21}Al_{0.51})(Cr_{2.60}Ti_{0.08}Al_{1.39})(Si_{5.34}Al_{0.61})O_{22}(OH)_{4.00} \cdot 1.97H_2O$;
[34] $(Ca_{7.63}Na_{0.17}K_{0.01})(Mn^{2+}_{2.75}Mg_{1.10})(Mn^{3+}_{4.50}Al_{1.87}Fe^{3+}_{1.61}Ti_{0.02})Si_{12.13}O_{39.71}(OH)_{16.29}$;
[35] $Ca_2(Fe^{2+}_{0.48}Fe^{3+}_{0.52})(Fe^{3+}_{0.94}Al_{0.06})_2Si_3O_{10.52}(OH)_{3.48}$;
[36] $(Ca_{8.8}Mn_{0.1})(Fe^{2+}_{2.7}Fe^{3+}_{1.2}Mg_{0.1})(Fe^{3+}_{7.2}Al_{0.6})Si_{12.7}O_{44.7}(OH)_{11.7}$;
[37] SiO_2 – 33.8(1) %; CaO – 61.6(1) %; H_2O – 4.6 %, close to theoretical composition;
[38] SiO_2 – 47.0 %; FeO – 0.17 %; MnO – 0.006 %, MgO – 0.1 %; CaO – 45 %; Na_2O – 0.2 %; BaO – 0.75 %; SrO – 0.03 %; ignition loss at 950 °C, 6.5 %;
[39] $Ca_3Si_3O_8(OH)_2$;
[40] $[Y_{2.70}Yb_{0.07}Er_{0.08}Dy_{0.05}(Lu,Gd,Tm,Ho)_{0.03}]Si_{3.06}O_{10}F_{0.97}(OH)_{0.03}$;
[41] natural sample;
[42] natural sample, Arizona, near Kingman;
[43] natural sample: SiO_2 – 29.88 %; Y_2O_3 – 63.35 %; Fe_2O_3 – 0.30 %, Al_2O_3 + BeO – 0.45 %; CaO – 0.49 %; MgO – 0.21 %; Na_2O – 0.26 %; SnO_2 – 0.23 %; H_2O – 2.08 %; CO_2 – 1.04 %; H, Ne, etc. – 1.40 %;

Table 4 (continued)

[44] natural sample, Vittore mine, Balangero, Italia; no complete composition is given; see also [15]
[45] natural sample, Mts. Parang, Romania, composition not mentioned;
[46] natural sample, Mts. Maramures, Romania, composition not mentioned;
[47] natural sample with Al/Si = 2.9 and some impurities; [48] $(Na,H)_2ZrSi_2O_7$ with Na/H = 5/1;
[49] SiO_2 – 48.61 %; Al_2O_3 – 0.06 %; FeO – 0.18 %; MnO – 0.006 %; MgO – 0.10 %; CaO – 44.83 %; Na_2O – 0.21 %; BaO – 0.77 %; SrO – 0.03 %; B_2O_3 – 0.001 %; ignition loss – 5.2 %;
[50] $Ca_9(Si_6O_{18}H_2)(OH)_8 \cdot 6H_2O$; [51] $Ca_9(Si_6O_{18}H_2)(OH)_8 \cdot 2H_2O$; [52] natural sample, California.

Table 5. Hyperfine parameters obtained by ^{57}Fe NGR studies.

Silicate[d]	T [K]	Site	δ[a] [mm/s]	ΔQ [mm/s]	DH [mm/s]	A %		Refs.
						^{57}Fe NGR	Rietveld analysis	
Balangeroite[44]	80	$Fe1^{2+}$	1.38	2.65	0.48	69.9		94D1
		$Fe2^{2+}$	1.27	2.98	0.48	10.3		
		$Fe1^{3+}$	0.54	0.68	0.48	9.3		
		$Fe2^{3+}$	0.70	1.00	0.48	10.5		
	295	$Fe1^{2+}$	1.12	2.31	0.44	69.9		
		$Fe2^{2+}$	1.02	2.77	0.44	10.3		
		$Fe1^{3+}$	0.56	0.49	0.44	9.3		
		$Fe2^{3+}$	0.62	1.06	0.44	10.5		
Pumpellyite[45]	RT	Fe^{2+}(X)	0.99(2)[b]	3.24(4)	0.48(2)	80(3)		97C1,
		Fe^{3+}(X)	0.34(4)[b]	1.23(8)	0.35(9)	7(5)		97C2
		Fe^{3+}(Y)	0.26(2)[b]	1.93(4)	0.36(5)	13(4)		
Pumpellyite[46]	RT	Fe^{2+}(X)	0.90(2)[b]	2.68(4)	0.34(3)	66(3)		97C1,
		Fe^{3+}(X)	0.35(4)[b]	1.04(6)	0.46(5)	18(4)		97C2
		Fe^{3+}(Y)	0.26(2)[b]	1.95(6)	0.27(4)	16(4)		
Pumpellyite[27]	77	Fe^{2+}	≅ 1.20			72		94A1
		Fe^{3+}	≅ 0.45			28		
	293	Fe^{2+}	1.12			66	69 (X-site)	
		Fe^{3+}	≅ 0.35			34	31 (Y-site)	
Pumpellyite[28]	77	Fe^{2+}	≅ 1.20			29		94A1
		Fe^{3+}	≅ 0.45			71		
	293	Fe^{2+}	1.12			27	34 (X-site)	
		Fe^{3+}	≅ 0.35			73	66 (Y-site)	
Pumpellyite[29]	77	Fe^{2+}	≅ 1.20			24		94A1
		Fe^{3+}	≅ 0.45			76		
	293	Fe^{2+}	1.03…1.09			23	30 (X-site)	
		Fe^{3+}	≅ 0.35			77	76 (Y-site)	
Okhotskite[34]		Fe^{3+}	0.39(2)	0.41(2)	0.31(2)	62(2)		87T1
		Fe^{3+}	0.34(2)	1.04(2)	0.35(2)	15(2)		
		Fe^{3+}(piemontite)[c]	0.35(2)	1.91(2)	0.33(2)	23(2)		

[a] relative to α-Fe; [b] relative to α-Fe_2O_3 + $Na_2[Fe(CN)_5NO] \cdot 2H_2O$; [c] piemontite was not possible to separate from okhotskite; [d] for composition see footnotes in Table 4.

Table 6. Data obtained from NMR studies.

Sample	T [K]	Nucleus	Site	δ_{iso} [ppm]	QCC[1)] [MHz]	OB[2)] [Hz]	DH[3)] [Hz]	η	Refs.
Zunyite[47)]	RT	^{27}Al	$^{[4]}$Al(Al_{13})	71.6(5)	0.8(5)	30	520	0	95D1
			$^{[6]}$Al(Al_{13})	8.9(5)	2.2(5)	280	900	0	
			$^{[4]}$Al(penta)	46.8(5)	0.5(5)… 1.0(5)	30	250	0	
Zunyite			$^{[4]}$Al(Al_{13})	72	0.6	20			84K1
			$^{[6]}$Al(Al_{13})	8	2.2	280			
Zunyite[47)]		^{29}Si	Q^1(1Si)	–96.6					95D1
			Q^4(4Si)	–128.2					

[1)] quadrupole coupling constant; [2)] second order quadrupole broadening at $B_0 = 11.7$ T; [3)] full width at half height at $B_0 = 11.7$ T; [47)] for composition see footnote in Table 4.

Table 7. Refractive indices.

Silicate[a)]	n_α	n_β	n_γ	$2V$°		Refs.
Davreuxite[4)]	1.660(5)	1.684(2)	1.690(2)	48(5)°	biaxial negative	84F1
Keldyshite[48)]	1.670		1.710	60° for red 78° for yellow 112° for blue	biaxial negative	62G1
Parakeldyshite[7)]	1.697	1.670	1.718	83°		73K1
Parakeldyshite[8)]	1.670	1.692	1.713	84°		77R1
Khibinskite[9)]	1.665	≅ 1.715	≅ 1.715	11°	biaxial negative	73K1
Medaite[10)]	1.77(1)	1.78(1)	1.80(1)	71° (calc.)	biaxial positive	81G1, 82G1
Tiragalloite[11)]	1.745(5)	1.751(3)	1.760(5)	38°…46°	biaxial positive	80G1
Johninnesite[20)]	1.6742(4)	1.6968(3)	1.6999(3)	41.9°	biaxial negative	86D1
Pumpellyite-(Mn^{2+})[22)]	1.752(2)	1.795(5)	1.800(5)	40°	biaxial negative	81K1
Shuiskite[33)]	1.725...1733	1.762...1772	1.769...1775	40°…50°	biaxial negative	81I1, 82F1
Okhotskite[34)]	1.782(5)	1.820(5)	1.827(5)	46(5)° (meas.) 46° (calc.)	biaxial negative	87T1
Julgoldite[36)]	1.776(4)	1.814(4)	1.836(4)	50°…70° 73° (calc.)	biaxial negative	71M1
Rustamite[37)]	1.640		1.651	–80°		65A1
Rosenhahnite[49)]	1.625(2)	1.640(2)	1.646(2)	–64(4)°		67P1
Thalenite[42)]	1.716	1.723	1.729	–69(2)°		86F1
Thalenite[43)]	1.725	1.733	≅ 1.738			86F1
Thalenite[41)]	1.717	1.736	1.746	–68°		72K1
Jennite[52)]	1.552(9)	1.564(3)	1.571(3)	–74° (calc.)		66C1

[a)] for compositions see footnotes in Table 4.

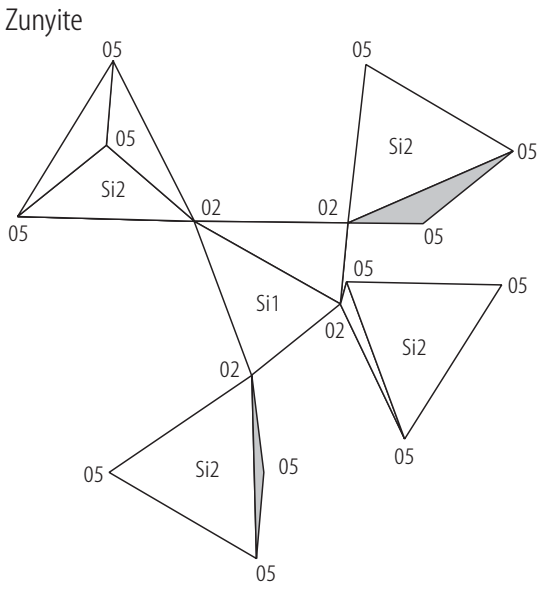

Fig. 1. Zunyite. The Si_5O_{16} pentamer [95D1].

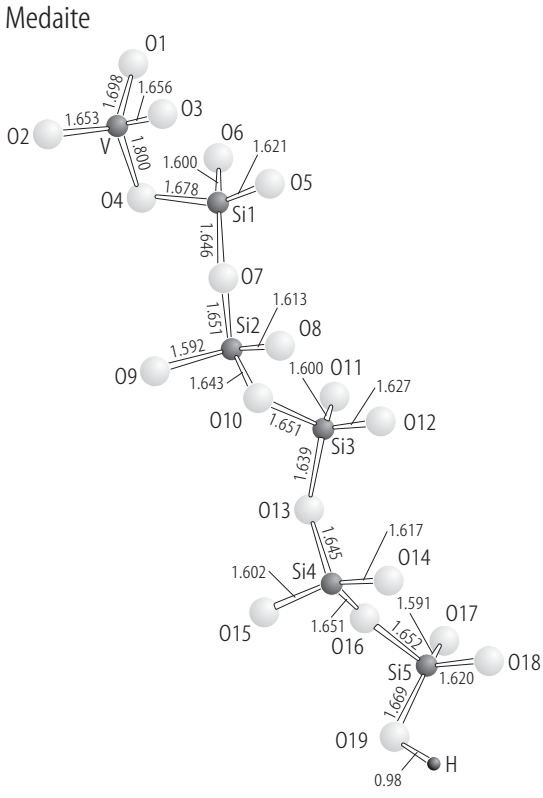

Fig. 3. Medaite. Conformation of the $[VSi_5O_{18}(OH)]^{12-}$ ion [82G1]. Bond lengths are in Å.

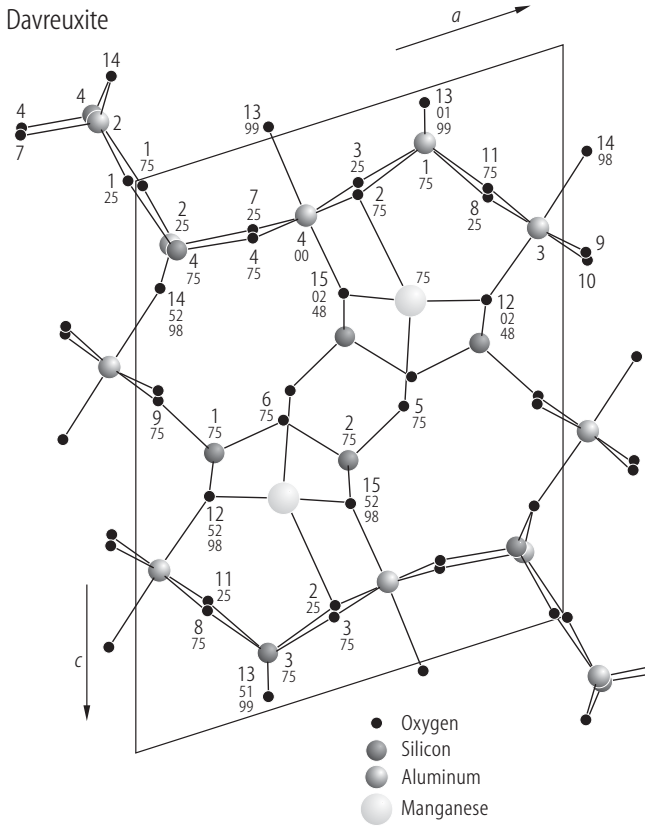

Fig. 2. Davreuxite. Projection of structure along [010]. The atom numbering (large numbers) corresponds to Table 2. The *y* coordinates multiplied by 100 are also given (small numbers) [84S1].

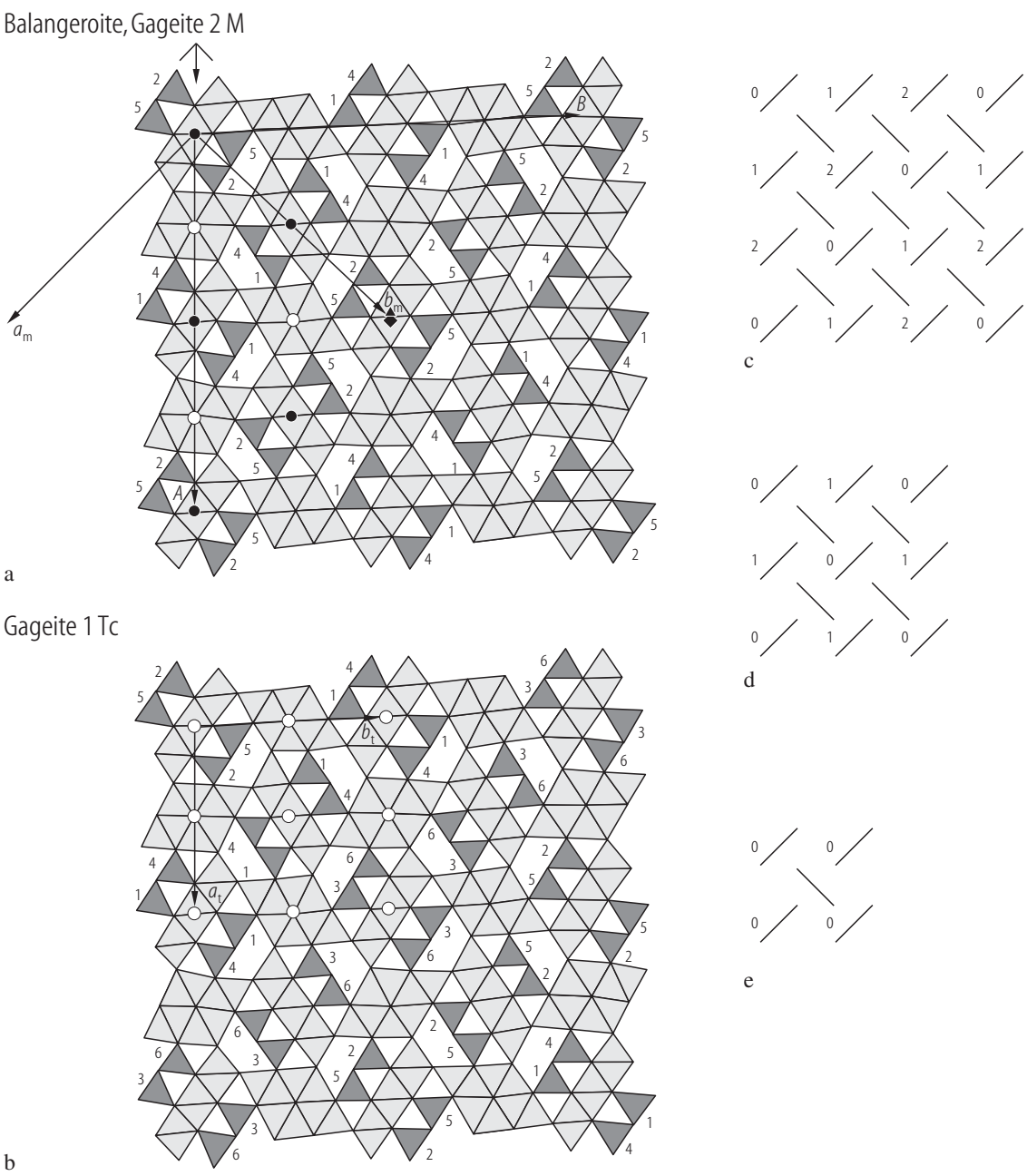

Fig. 4. Balangeroite and gageite 2M **(a)** and gageite 1 Tc **(b)**: crystal structures. The digits give the height, in C/6 units, of the different tetrahedral chains with reference to the bridging oxygen atoms. The symmetry elements are indicated. In **(a)** both the double $A \times B \times C$ cell and primitive $a_m \times b_m \times c_m$ cell are indicated. In **(b)** is plotted the primitive triclinic cell. In **(c, d, e)** the schematic drawings of the different polytypes are given, with indications, in C/3 units, of the relative heights of the T-**O**-T modules; **(c)** triclinic form, **(d)** monoclinic form, **(e)** hypothetical orthorhombic form [87F1].

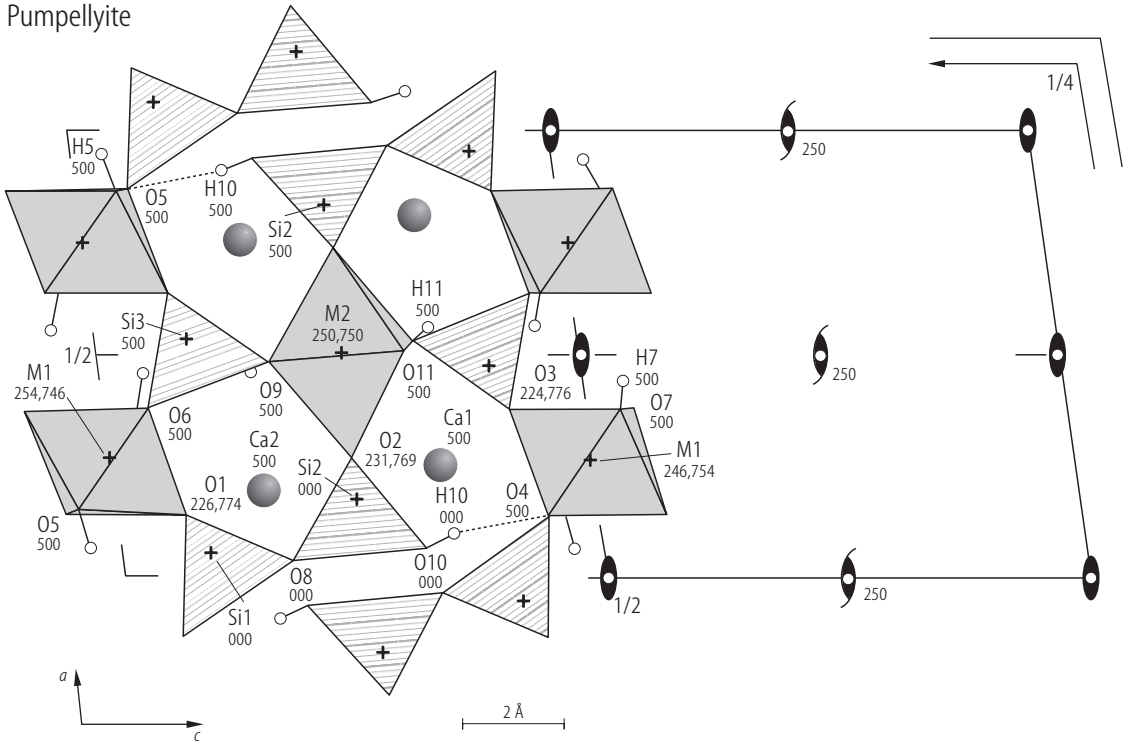

Fig. 5. Pumpellyite. View parallel to [010]. The heights of the atoms are indicated in 1000 *y*. The elements of symmetry are given in half of the unit cell [85Y1].

For Fig. 6 see next page

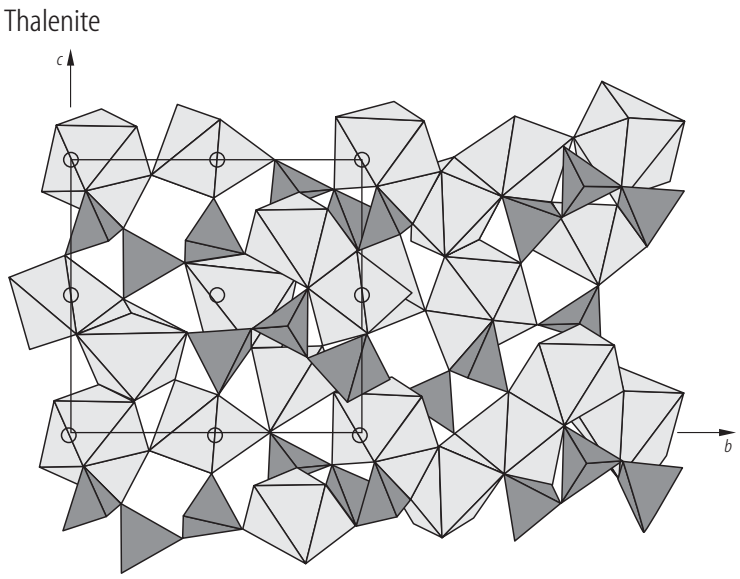

Fig. 7. Thalenite. *yz* projection. On the right-hand side of the drawing the dark speckle denotes a fragment of the structure at height $x \cong 0.4$; the part on the left corresponds to $x \cong 0.8$ [88Y1].

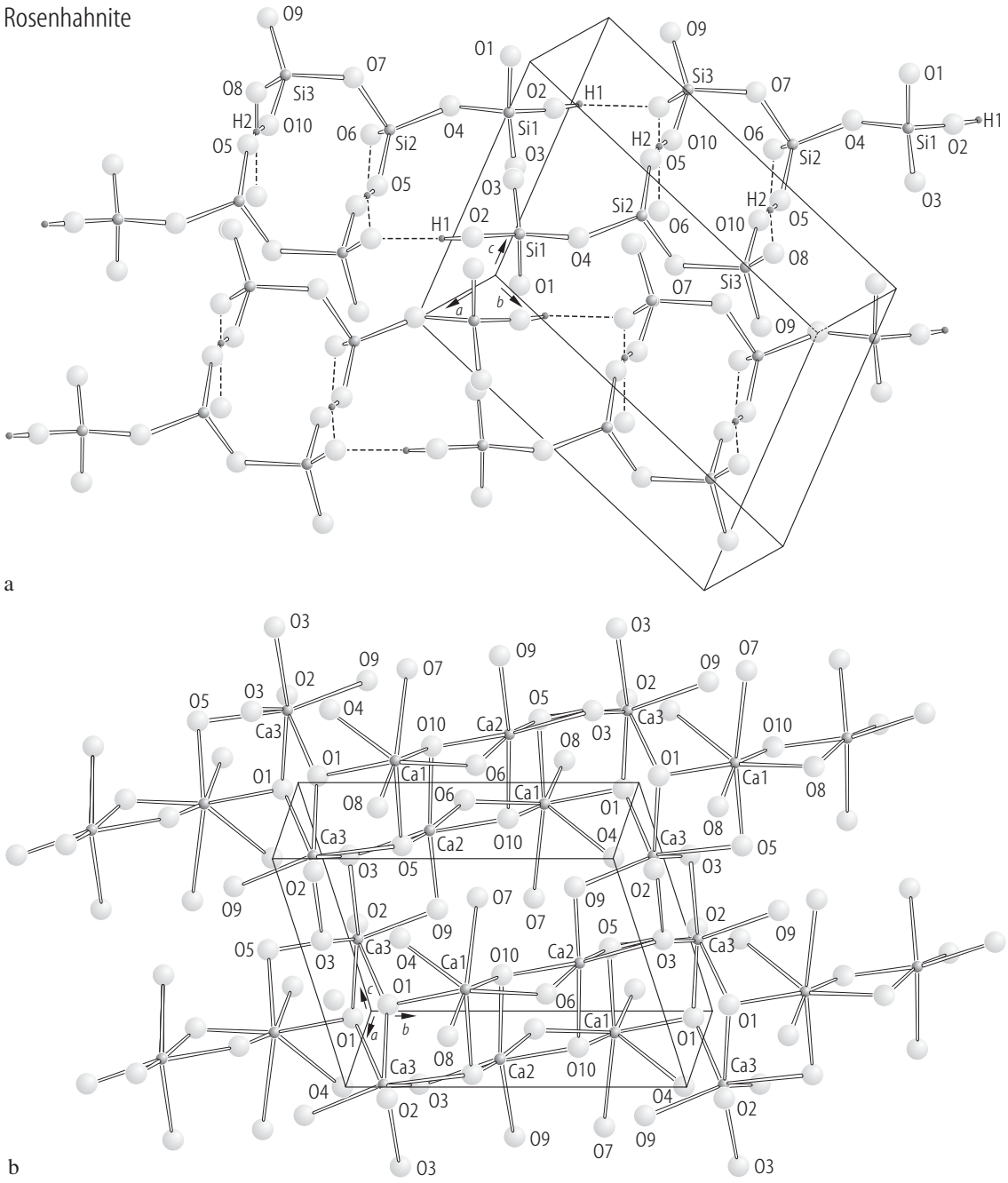

Fig. 6. Rosenhahnite. Partial view of the structure showing. **(a)** Trisilicate groups hydrogen bonded through H1 into linear chains. The hydrogen atom H2 bonds two adjacent trisilicate groups accross a symmetry center into dimers. **(b)** Calcium polyhedra [77W1].

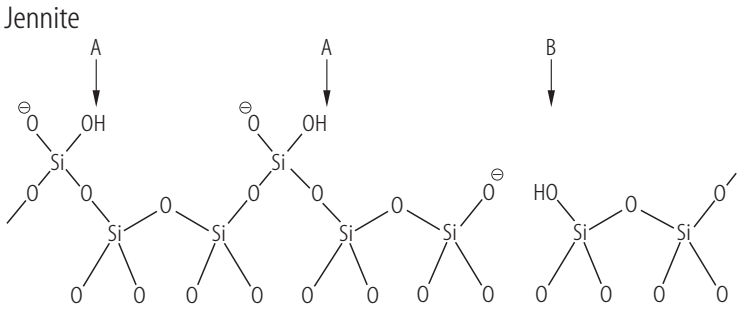

Fig. 8. Jennite. Silicate chain present in jennite and 1.4 nm tobermorite, showing the probable positions of the H atoms (A) and suggested modification (B) by the omission of a bridging tetrahedron [86T1].

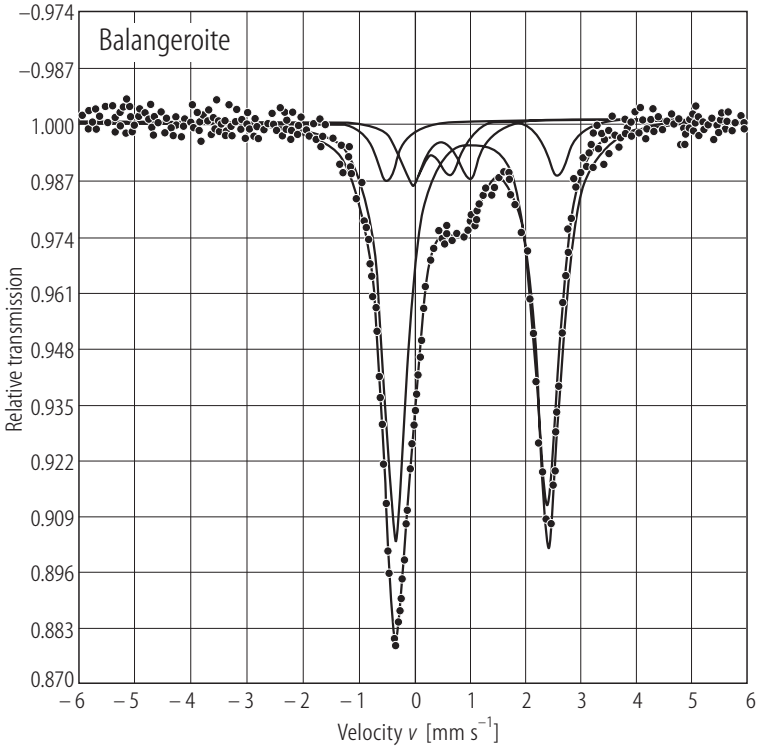

Fig. 9. Balangeroite[44]. ^{57}Fe NGR spectrum at 80 K [94D1].

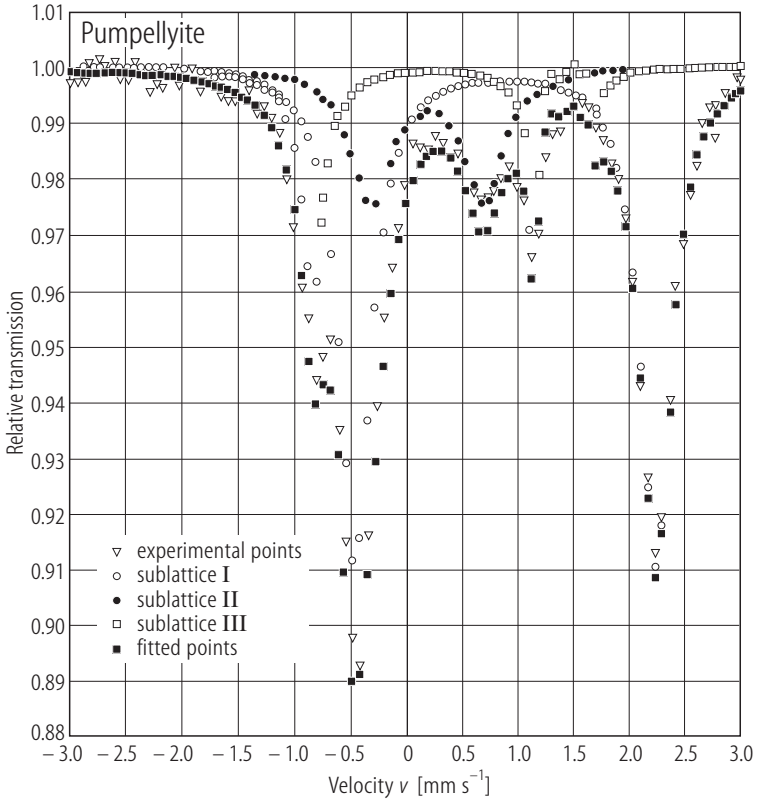

Fig. 10. Pumpellyite[46]. ^{57}Fe NGR spectrum at room temperature [97C2].

For Fig. 11 see next page

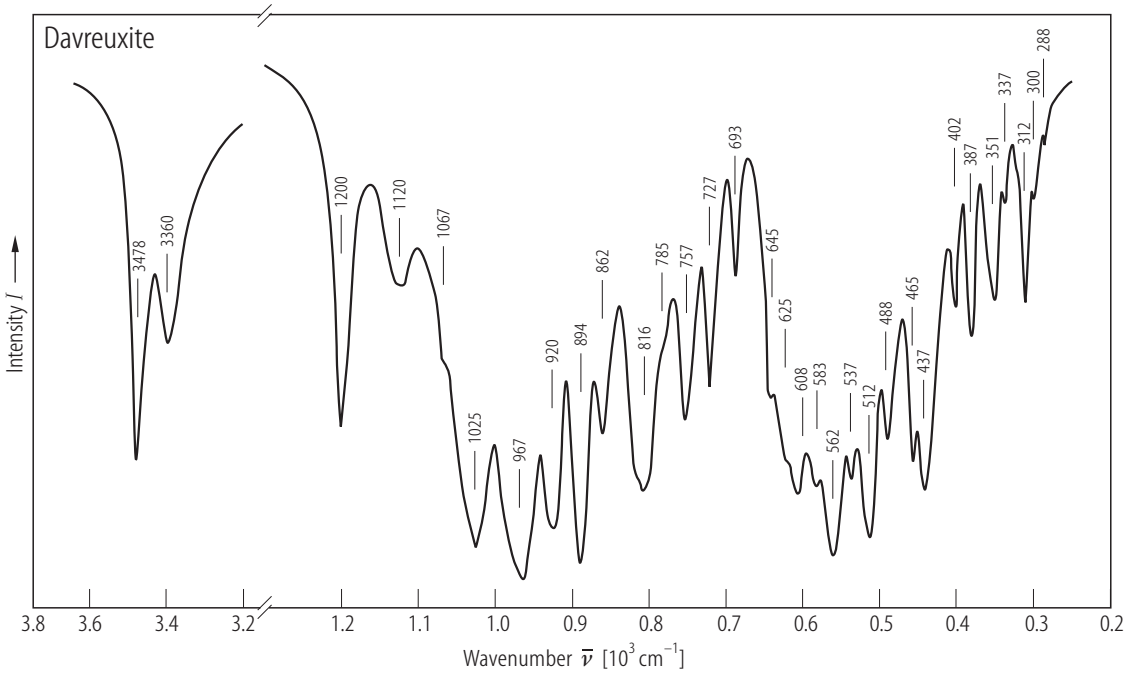

Fig. 12. Davreuxite[4]. Infrared spectrum [84F1].

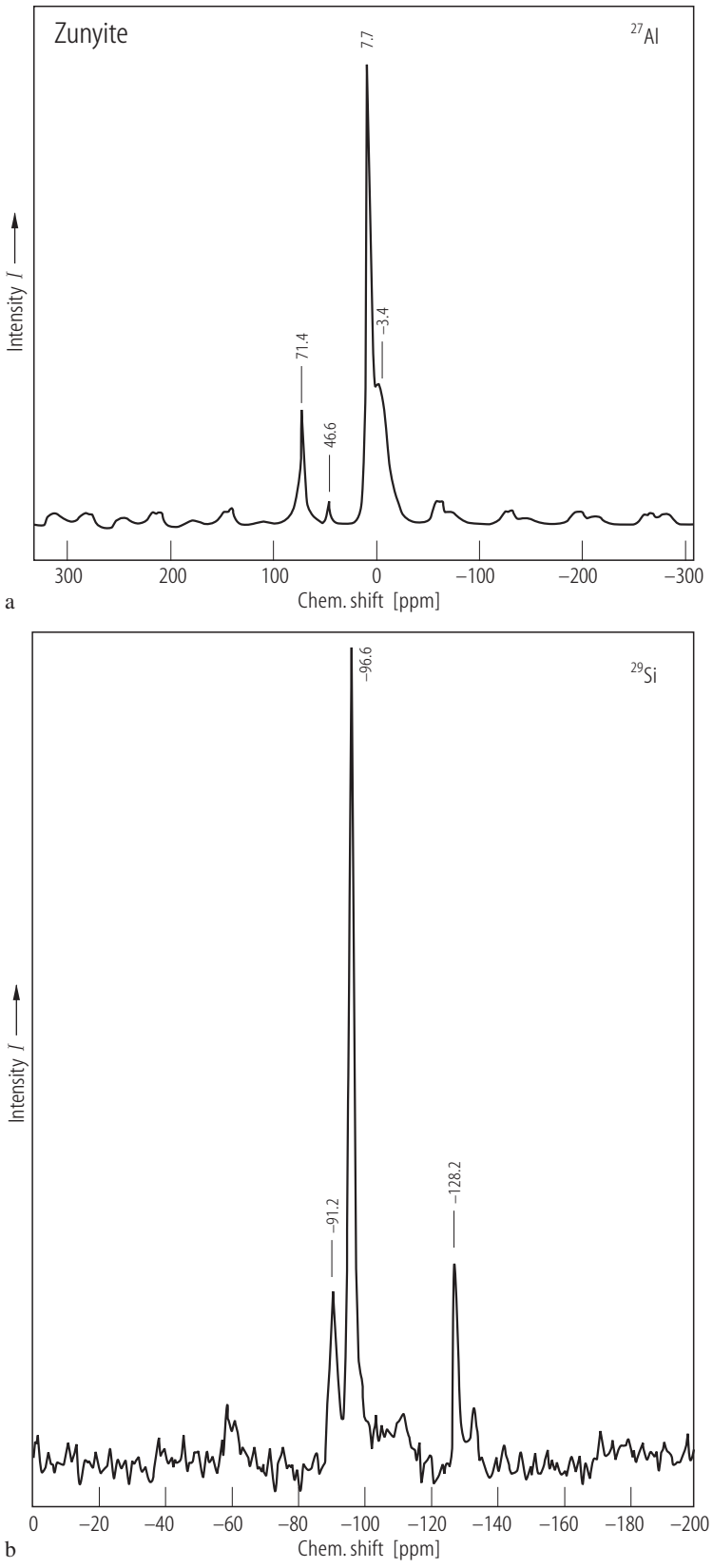

Fig. 11. Zunyite[47]. ^{27}Al **(a)** and ^{29}Si **(b)**. MAS NMR spectra at a magnetic field of 11.7 T [95D1].

References for 8.1.2.8

25P1 Palache, C., Vassar, H.E.: Am. Mineral. 10 (1925) 412
33P1 Pauling, L.: Z. Kristallogr. 84 (1933) 442
56D1 Dornberger-Schiff, K.: Acta Crystallogr. 9 (1956) 593
60K1 Kamb, W.B.: Acta Crystallogr. 13 (1960) 15
62G1 Gerasimovskii, V.I.: Dokl. Akad. Nauk SSSR 142 (1962) 916
62T1 Turco, G.: Bull. Soc. Fr.. Mineral. Cristallogr. 85 (1962) 407
65A1 Agrell, S.O.: Mineral. Mag. 34 (1965) 1
65G1 Gottardi, G.: Tschermaks Mineral. Petrogr. Mitt. 10 (1965) 115
66C1 Carpanter, A.B., Chalmers, R.A., Gard, J.A., Speakman, K., Taylor, H.F.W.: Am. Mineral. 51 (1966) 56
67B1 Bancroft, G.M., Maddock, A.G., Burns, R.G.: Geochim. Cosmochim. Acta 31 (1967) 2219
67P1 Pabst, A., Gross E.B., Alfors, J.T.: Am. Mineral. 52 (1967) 336
68M1 Moore, P.B.: Am. Mineral. 53 (1968) 309
68M2 Moore, P.B.: Am. Mineral 53 (1968) 1418
69G1 Galli, E., Alberti, A.: Acta Crystallogr. B25 (1969) 2276
69K1 Khomyakov, A.P., Kazakova, M.E., Voronkov, A.A.: Dokl. Akad. Nauk SSSR 189 (1969) 166
69M1 Moore, P.B.: Am. Mineral. 54 (1969) 1005
71A1 Allmann, R., Donnay, G.: Acta Crystallogr. B27 (1971) 1871
71B1 Baur, W.H.: Am. Mineral. 56 (1971) 1573
71M1 Moore, P.B.: Lithos 4 (1971) 93
72D1 Dornberg-Schiff, K., Fichtner, K.: Krist. Tech. 7 (1972) 1035
72K1 Kornev, A.N., Batalieva, N.G., Maksimov, B.A., Ilyukhin, V.V., Belov, N.V.: Dokl. Akad. Nauk SSSR 202 (1972) 1324 (Sov. Phys. Dokl. 17 (1972) 88)
73A1 Allmann, R., Donnay, G.: Mineral. Mag. 39 (1973) 271
73D1 Dollase, W.A.: Z. Kristallogr. 138 (1973) 41
73J1 Jeffrey, J.W., Lindley, P.F.: Nature 241 (1973) 42
73K1 Khomyakov, A.P., Voronkov, A.A.: Tr. Mineral. Muz. Akad. Nauk SSSR 22 (1973) 215
73L1 Louisnathan, S.J., Gibbs, G.V.: Am. Mineral. 58 (1973) 138
73P1 Passaglia, E., Gottardi, G.: Can. Mineral. 12 (1973) 219
75D1 Dollase, W.A.: Am. Mineral. 60 (1975) 257
76F1 Fransolet, A.M., Bourguignon, P.: C. R. Acad. Sci (Paris) 283D (1976) 295
77G1 Gard, J.A., Taylor, H.F.W.: Am. Mineral. 62 (1977) 365
77R1 Raade, G., Mladeck, M.H.: Can. Mineral. 15 (1977) 102
77W1 Wan, C., Ghose, S., Gibbs, G.: Am. Mineral. 62 (1977) 503
79D1 Dunn, P.J.: Am. Mineral. 64 (1979) 1056
79G1 Gramaccioli, C.M., Pilati, T., Liborio, G.: Acta Crystallogr. B35 (1979) 2287
80C1 Chieh, C.: Acta Crystallogr. A36 (1980) 819
80G1 Gramaccioli, C.M., Griffin, W.L., Mottana, A.: Am. Mineral. 65 (1980) 947
80H1 Hara, N., Inoue, N.: Cem. Concr. Res. 10 (1980) 67
80S1 Schiffmann, P., Liou, J.G.: J. Petrol. 21 (1980) 441
81G1 Gramaccioli, C.M., Liborio, G., Pilati, T.: Acta Crystallogr. B37 (1981) 1972
81I1 Ivanov, O.K., Arkhangelskaya, V.A., Miroshnikova, L.O., Shilova, T.A.: Urals. Zap. Vses. Mineral. Ova. 110 (1981) 508
81K1 Kato, A., Matsubara, S., Yamamoto, R.: Bull. Mineral. 104 (1981) 396
81O1 Offler, R., Baker, C.K., Gamble, J.: Contrib. Mineral. Petrol. 76 (1981) 171
82B1 Baur, W.H., Ohta, T.: Acta Crystallogr. B38 (1982) 390
82F1 Fleischer, M., Chao, G.Y., Mandarino, J.A.: Am. Mineral. 67 (1982) 854
82G1 Gramaccioli, C.M.: Am. Mineral. 67 (1982) 85
83C1 Compagnoni, R., Ferraris, G., Fiora, L.: Am. Mineral. 68 (1983) 214
83G1 Grimmer, A.R., Von Lampe, F., Tarmak, M., Lippmaa, E.: Chem. Phys. Lett. 97 (1983) 185
84F1 Fransolet, A.M., Abraham, K., Sahl, K.: Am. Mineral. 69 (1984) 777
84K1 Kunwar, A.C., Thompson, A.R., Gutowsky, H.S., Oldfield, E.: J. Magn. Res. Commun. 60 (1984) 467

84M1 Mellini, M., Merlino, S., Pasero, M.: Phys. Chem. Miner. 10 (1984) 99
84S1 Sahl, K., Jones, P.G., Sheldrick, G.M.: Am. Mineral. 69 (1984) 783
85B1 Brown, I.D., Altermatt, D.: Acta Crystallogr. B41 (1984) 244
85D1 Deer, W.A., Howie, R.A., Zussmann, J.: in Rock Forming Minerals, Vol. 1B: Disilicates and Ring Silicates, 2nd edition, Longman, Harlow, (1985) p. 201
85V1 Voloshin, A.V., Pakhomovskii, Ya. A., Tyusheva, F.N.: Mineral. Zh. 7 (1985) 79
85Y1 Yoshiasa, A., Masumoto, T.: Am. Mineral. 70 (1985) 1011
86D1 Dunn, P.J., Peacor, D.R., Su, S.C., Nelen, J.A., Von Knorring, O.: Mineral. Mag. 50 (1986) 667
86F1 Fitzpatrick, J., Pabst, A.: Am. Mineral. 71 (1986) 188
86H1 Hesse, K.F., Stimpel, G.: Z. Kristallogr. 177 (1986) 143
86S1 Schreyer, W., Maresch, W.W., Medenbach, O., Baller , T.: Nature 321 (1986) 510
86T1 Taylor, H.F.W.: J. Am. Ceram. Soc. 69 (1986) 464
87F1 Ferraris, G., Mellini, M., Merlino, S.: Am. Mineral. 72 (1987) 382
87S1 Schreyer, W., Maresch, W.V., Baller, T.: Terra Cognita 7 (1987) 385
87T1 Togari, K., Akasaka, M.: Mineral. Mag. 51 (1987) 611
88Y1 Yakubovich, O.V., Voloshin, A.V., Pakhomovskii, Ya.A., Simonov, M.A.: Kristallografiya. 33 (1988) 605 (Sov. Phys. Crystallogr. 33 (1988) 365)
91A1 Artioli, G., Sacchi, M., Balerna, A., Burattini, E., Simeoni, S.: Neues Jahrb. Mineral. Monatsh. 9 (1991) 413
91B1 Belluso, E., Ferraris, G.: Eur. J. Mineral. 3 (1991) 559
91D1 Dasgupta, S., Chakraborti, S., Sengupta, P., Bhattacharya, P.K., Banerjee, H., Roy, S., Fukuoka, M.: Am. Mineral. 76 (1991) 241
91N1 Nickel, E.H., Nichols, M.C.: Mineral Reference Manual, Van Norstrand Reinhold, 1991
91P1 Pasero, M., Reineke, T.: Eur. J. Mineral. 3 (1991) 819
91S1 Sherriff, B.L., Grundy, H.D., Hartman, J.S.: Eur. J. Mineral. 3 (1991) 751
92F1 Furrer, G., Ludwig, C., Schindler, P.W.: J. Colloid Interface Sci. 149 (1992) 56
92P1 Pan, Y., Fleet, M.E.: Can. Mineral. 30 (1992) 153
94A1 Artioli, G., Geiger, C.A.: Phys. Chem. Miner. 20 (1994) 443
94D1 Deriu, A., Ferraris, G., Belluso, E.: Phys. Chem. Miner. 21 (1994) 222
95A1 Artioli, G., Quartieri, S., Deriu, A.: Can. Mineral. 33 (1995) 67
95D1 Dirken, P.J., Kentgens, A.P.M., Nachtegaal, G.H., Van Der Eerden, M.J., Jansen, J.B.H.: Am. Mineral. 80 (1995) 39
96A1 Artioli, G., Pavese, A., Bellotto, M., Collins, S.P., Lucchetti, G.: Am. Mineral. 81 (1996) 603
96C1 Coombs, D.S., Kawachi, Y., Ford, P.B.: J. Metamorph. Geol. 14 (1996) 185
97A1 Akasaka, M., Kimura, Y., Omori, Y., Sakakibara, M., Shinno, I., Togari, K.: Mineral. Petrol. 61 (1997) 181
97C1 Constntinescu, S., Udubasa, Gh., Calogero, S.: J. Phys. (France) 7 (1997) 777
97C2 Constntinescu, S., Udubasa, Gh., Calogero, S.: Rom. J. Phys. 42 (1997) 359
98F1 Fockenberg, T.: Am. Mineral. 83 (1998) 220
99A1 Artioli, G., Fumagalli, P., Poli, S.: Am. Mineral. 84 (1999) 1906
00G1 Gottschalk, M., Fockenberg, T., Grevel, K.D., Wunder, B., Wirth, R., Schreyer, W., Maresch, W.V.: Eur. J. Mineral. 12 (2000) 935.